Ion Specificity from Small Molecules to Oligomers and Beyond Amide-Based Macromolecules

A THESIS SUBMITTED TO

THE GRADUATE SCHOOL OF ENGINEERING AND SCIENCE

OF

BILKENT UNIVERSITY

IN PARTIAL FULFILLMENT OF THE REQUIREMENTS FOR

THE DEGREE OF

MASTER OF SCIENCE

IN

CHEMISTRY

BY

SOBIA FAROOQ

JANUARY 2024

ION SPECIFICITY FROM SMALL MOLECULES TO OLIGOMERS AND BEYOND AMIDE-BASED MACROMOLECULES

BY SOBIA FAROOQ
JANUARY 2024

We certify that we have read this thesis and that in our opinion it is fully adequate, in scope and in quality, as a thesis for the degree of Master of Science.

_____

Emrah Özensoy (Advisor)

_____

Halil İbrahim Okur (Co-Advisor)

_____

Fahri Alkan

_____

Zafer Say

Approved for the Graduate School of Engineering and Science:

_____

Orhan Arıkan

Director of the Graduate School

ABSTRACT

ION SPECIFICITY FROM SMALL MOLECULES TO OLIGOMERS AND BEYOND AMIDE-BASED MACROMOLECULES

SOBIA FAROOQ

M.S. in Chemistry

Advisor: EMRAH ÖZENSOY Co-Advisor HALİL İBRAHİM OKUR

JANUARY 2024

Presence of ions in aqueous solution regulate the properties of molecules in the same aqueous environment. Such alteration processes are mainly dependent on the concentration and the identity of ions. In this thesis, two parts of ion specific effects were aimed to be explored. First the synthesis and characterization of PNIPAM oligomers by using both reversible addition-fragmentation chain transfer (RAFT) and radical polymerization methods will be shown. Both of these methods give the control over molecular size of the polymer. Oligomers with charged and neutral end group were synthesized to comparatively investigate ion specific effect. These oligomers were also systematically characterized by using various analytical techniques such as phase transition temperature measurement, ^{1}H-NMR and Gel permeation chromatography (GPC). Such oligomers were employed to investigate the specific ion effects via the salt influence on the Lower Critical solution temperature (LCST). By employing two sodium salts; NaCl (strongly hydrated) and NaSCN (weakly hydrated), it was found that strongly hydrated anions salt-out both charged and neutral oligomers, whereas weakly hydrated anions increase the phase transition temperature with a salting in mechanism. By empirical modeling with a Langmuir-type binding isotherm, a weak binding with a dissociation constant K_D = 0.57 M for charged and K_D = 1.13 M for neutral oligomers were demonstrated.

The second part of this thesis focused on the specific ion effects beyond amide-based macromolecules i.e. hydroxypropyl cellulose (HPC) as a model for sugar-based macromolecules. Eight sodium salts were employed to demonstrate the entire Hofmeister series. Namely; NaSCN, NaI, $NaNO_3$, $NaClO_4$ NaCl, Na_2SO_4, Na_2CO_3, NaH_2PO_4 were measured on the phase transition temperature and ^{1}H-NMR measurements. Salts of weakly hydrated anions; NaSCN, NaI, $NaClO_4$ and $NaNO_3$ showed a salting in mechanism and demonstrate a non-monotonic phase transition

behavior. In contrast, salts of strongly hydrated anions; NaCl, Na_2SO_4, NaH_2PO_4 and Na_2CO_3 showed salting out mechanism with a monotonic decrease in the phase transition temperature. Additionally, the site-specific ion-macromolecule interaction was studied by ^{1}H-NMR, and Correlation Spectroscopy (2D-COSY) NMR measurements. Although, the exact binding site cannot be specified, it was concluded that the ion binding site is at the side-chain hydroxypropyl groups and that yields the salting-in effect that was observed for the weakly-hydrated anions.

Keywords: Macromolecules, Oligomers, Specific Ion Effects, Hydroxypropyl Cellulose, PNIPAM, RAFT Polymerization

ÖZET

KÜÇÜK MOLEKÜLLERDEN OLİGOMERLERE VE AMİT-BAZLI MAKROMOLEKÜLLERİN ÖTESİNDE İYON SPESİFİK ETKİLERİ

SOBIA FAROOQ

Kimya | Yüksek Lisans

Danışman: EMRAH ÖZENSOY

İkinci Danışman: HALİL İBRAHİM OKUR

Ocak 2024

Sulu çözeltilerde bulunan iyonlar, aynı sulu ortamdaki moleküllerin özelliklerini düzenler. Bu değişim süreçleri, başlıca iyonların konsantrasyonuna ve kimliğine bağlıdır. Bu tezde, iyon spesifik etkilerinin iki farklı alanı araştırılmıştır. İlk olarak, hem tersinir katılma-ayrışma zincir transfer (RAFT) hem de radikal polimerizasyon yöntemleri kullanılarak PNIPAM oligomerlerinin sentezi ve karakterizasyonu gerçekleştirildi. Bu yöntemler, sentezlenen polimerin moleküler boyutu üzerinde kontrol sağlar. Yüklü ve nötr uç grupları içeren oligomerler, iyon spesifik etkilerini karşılaştırmalı olarak incelemek için sentezlendi. Bu oligomerler, faz değişim sıcaklığı ölçümleri, ^{1}H-NMR ve jel permeasyon kromatografisi (GPC) gibi çeşitli analitik teknikler kullanılarak sistemli bir şekilde karakterize edildi. Bu oligomerler, tuzun faz değişim sıcaklığı üzerindeki etkisini incelemek için kullanıldı (LCST). İki klorür tuzu, NaCl (güçlü hidratlanmış) ve NaSCN (zayıf hidratlanmış) kullanılarak; güçlü hidratlanmış anyonların hem yüklü hem de nötr oligomerleri çözünürlüğünü azalttığı, zayıf hidratlanmış anyonların ise faz değişim sıcaklığını artırarak, oligomer çözünürlüğünü arttırdığı gösterildi. Langmuir bağlanma izoterimi ile ampirik modelleme kullanılarak, yüklü oligomerler için K_D = 0.57 M ve nötr oligomerler için K_D = 1.13 M olan zayıf bir iyon bağlanması gösterildi.

Bu tezin ikinci kısmı, amid temelli makromoleküller ötesinde spesifik iyon etkilerine odaklandı, şeker bazlı makromoleküller için bir model olan hidroksipropil selüloz (HPC) kullanıldı. Hofmeister serisini göstermek için sekiz farklı sodyum tuzu kullanıldı. Yani; NaSCN, NaI, $NaNO_3$, $NaClO_4$, NaCl, Na_2SO_4, Na_2CO_3, NaH_2PO_4, faz değişim sıcaklığı ve ^{1}H-NMR ölçümleri üzerinde kullanıldı. Zayıf hidratlanmış anyon tuzları; NaSCN, NaI, $NaClO_4$ ve $NaNO_3$, makromolekül çözünürlüğünü artıran bir mekanizma ile monotonik olmayan bir faz değişim

davranışı sergiledi. Buna karşılık, güçlü hidratlanmış anyon tuzları; NaCl, Na_2SO_4 NaH_2PO_4 ve Na_2CO_3, faz geçiş sıcaklığında monotonik bir azalmayla gösterdi. Buna ek olarak, iyon-makromolekül etkileşiminin bölgeye özgü olarak ^{1}H-NMR ve 2D-COSY NMR ölçümleri ile incelenmiştir. Direk bağlanma bölgesi belirlenemese de, iyon bağlanma yerinin yan-zincir hidroksipropil gruplarında olduğu ve bu durumun zayıf hidratlanmış anyonlarda gözlemlenen makromolekül çözünürlük artışı gösterdiği sonucuna varılmıştır.

Anahtar kelimeler: Makromoleküller, Oligomerler, Spesifik İyon Etkileri, Hidroksipropil Selüloz, PNIPAM, RAFT Polimerizasyonu.

ACKNOWLEDGEMENT

Reflecting on the three years of turbulent journey encompassing successes and failures, in particular I want to express sincere gratitude to my co-advisor Dr. Halil İbrahim Okur. His courteous demeanor, profound insights and vast scientific matters, coupled with his motivational support during challenging times, have had a significant impact in shaping my development as a researcher. Hocam! Grateful for your invaluable guidance. Additionally, I extend my heartfelt appreciation for chairman Department of Chemistry and my advisor Prof. Emrah Özensoy for his support.

I would also like to thanks the whole faculty of Department of Chemistry, especially to Prof. Omer Dag. His kindness, honesty and integrity is an inspiration for me that I wholeheartedly aim to adopt in my teaching career.

I wish to thank each member of the Okur Lab. The teamwork, encouragement and collaborative spirit of the group have greatly enhanced my research experience. I wish all current and future members the best!

I would like to thank Prof. Emrah Ozensoy, Dr. Fahri Alkan and Dr. Zafer Say for graciously be part of my thesis committee, whose constructive feedback and valuable discussion, markedly enhanced the quality of my work.

To my family: especially to my parents, your unconditional love, support and blessings have enabled me to overcome life's hurdles and reach the position where I am today. May your love and best wishes always accompany me on my life's Journey.

To all my friends, and specially to Momil, Rashid, Badar & Najeeb. Thank you for providing me motivation as well as invaluable emotional support. I feel fortunate to have you all in my life, the imprints of our connections will always stays in our hearts.

A special thanks to Prof, Şefik Süzer, the former chairman of Department of Chemistry, thank you for giving me the chance to be here.

It would be unfair to conclude this acknowledgement without thanking the writer of this work, I am not sure either this work is her failure or success but indeed she is courageous and have indomitable spirit.

Table of Contents

List of Figures

List of Tables

Chapter 1-Introduction

The physicochemical properties of a solution and molecules solvated inside are directly influenced by solvent molecules, ions and small molecules present in it. Electrolytes including acids, bases and salts are main components of the physiological system and regulate and stabilize proteins, enzymes[1-12] and cells[13], balance level of acidity as well[14] and fluid retention[15]. In most of these effects electrolytes are not only dependent on concentration and charge of ions as explained by theories such as Debye-Hückel theory but rely on their identity. For instance, potassium fluoride (KF) is vicious to humans, whilst potassium iodide (KI) is employed to cure hypothyroidism; clearly the identity and of course the concentration of the anion is important here. Numerous phenomena, in which the ion's identity is essential to determine the properties of a system, are generally referred to as specific ion effects (SIEs). First systematic studies on SIEs were performed more than 130 years ago by Lewith and Hofmeister between 1887 and 1891. In these early efforts, the first ionic series based on their abilities to precipitate proteins from blood serum and egg white in aqueous solutions were demonstrated.[16,17] A generic ion specific series can be seen as follows.

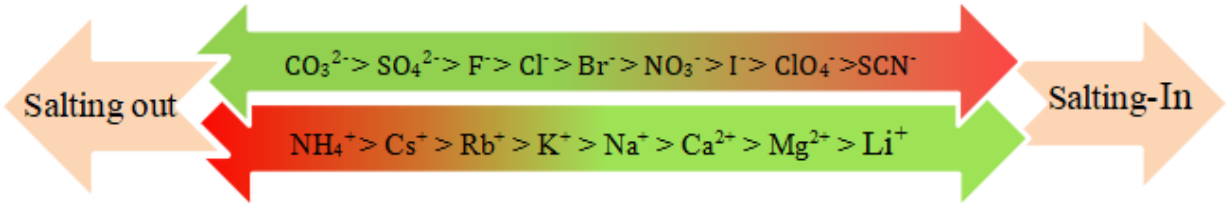

Figure 1: The recurring generic Hofmeister ion series top for anions and bottom for cations in play for numerous aqueous phase phenomena.

In this series ions on the right-hand side are associated with the phenomenon termed as salting in while those on the left hand side are referred to as contributing to salting out. Salting in involves increased solubility of molecules such as proteins, with the addition of specific salts while salting out refers to reduced solubility, often at high concentrations, leading to precipitation or aggregation. The specific ion effect which is commonly known as Hofmeister effect as well has been consistently observed in diverse biological, polymers and non-aqueous systems and influences diverse phenomena such as surface tension[18], zeta potentials[19], buffer[20],

thermoresponsive polymer behaviors[21-23], ion-binding to proteins[24] and membranes[25], membrane transport[26], molecular forces[27,28], viscosity[29-33], enzyme activity[1-12], bacterial growth[34], bubble stability[35], and others[36,37].

In this chapter, we will discuss the influence of ions on diverse domains, encompassing aqueous and non-aqueous solutions, as well as the air-water interface. Furthermore, a comprehensive examination of the influence of ions on solutes will be undertaken, and how they affect solutes in solutions - ranging from small molecules to large macromolecules will be delivered.

1.1. Aqueous Ion Specific Effects

The origin of Hofmeister effect can be tracked back to the phenomenon of solubilization of egg proteins in water mediated salts solutions. The significant findings have far reaching impacts and introduce the recurring trends in ions' propensity to precipitate various solutes. In earlier attempts on explaining the mechanism for the Hofmeister series was proposed [17] based on the solution behavior of ions that arose from their ability to adsorb water. Consequently, ions are categorized as kosmotropes (creating order) and chaotropes (disrupting order), and the Hofmeister series orders ions from the most kosmotropic one to chaotropic ones. Ions with kosmotropic character causes protein precipitation (salt-out), while chaotropic ones induce protein solubilization (salt-in). Numerous models and mechanisms have been proposed to expound the underlying fundamentals of the Hofmeister effect. Cavity models[36,37] focus on the ion's influence on solvent, with Melander and Horváth's model[36] linking salting-out behavior to ion surface tension increments and a protein salting-out constant. Pica and Graziano[38,39] utilized solvent-excluded volume effects to describe poly (*N*-isopropylacrylamide) (PNIPAM) hydration. Baldwin's model[40] suggested ion interactions at non-polar functional groups for protein precipitation and interactions at peptide groups for salting-in. In polymer systems, Rogers *et al.*[41] proposed that weakly hydrated ions bind preferentially to the center of macromolecular chains. Collins[42] introduced the Law of Matching Water Affinities (LMWA), considering association of ion pairs and their enthalpies of hydration. Lo Nostro and Ninham[14] proposed that the Hofmeister effect results from three essential aspects i) the pairing between cation–anion and their interactions with both cosolutes and solvent molecules, ii) 'Local' interactions between ions and cosolutes drive specific ion adsorption, influenced by many-body quantum mechanical dispersion forces often overlooked in standard theories. These interactions, along with specific hydration, depend on the dielectric attribute of the

ion, solvent and cosolutes, and iii) additional phenomena contribute to anomalies such as reordering the series of ionic efficacy and series inversions.

1.1.1. Solvation of Ions in Aqueous Medium

The origin of specific ion effects (SIEs) in aqueous electrolytes has long been considered to be mainly related to the local solvation environment of the dissolved ions. Neutron diffraction experiments[43] supported the Hofmeister effect which is the result of protein and dissolved salts competing for water, other experiments such as X-ray absorption spectroscopy[44] indicate that addition of salt may alter the behavior of hydrogen bonds in water. According to many other methods, ions might not have much of an effect on water other than the first solvation layer which surrounds them. However, there is still disagreement- some studies suggest[45,46] that ions that are well hydrated cloud affect the arrangement of water molecules beyond the initial solvation layer.

Classical models on salt interactions in aqueous solutions, such as Born energies[47,48], Debye–Huckel (DH)[49], and Derjaguin–Landau–Verwey–Overbeek (DLVO)[50-52], were proposed to explain solvation and solution behavior of ions. Since all these derivations adapted a continuum model to describe solvent medium and point charges for ions, they cannot capture the SIEs. DH theory, assuming non-polarizable point charges and complete ion dissociation, is limited to dilute environments, while extended models improve accuracy up to 0.1 M. Specific ion interaction theory and the Pitzer Method[53] extend predictions to higher concentrations but rely on DH theory and require empirical parameters. One can argue that DH theory's early success contributes to a limited understanding of electrolyte solutions at higher concentrations (> 0.1 molar), emphasizing the need for more advanced theoretical treatments, considering ion properties beyond charge and size.[54]

1.1.2. Ion effect in solution-insight from ion properties and Hofmeister Series.

The influence of ions on a system is correlated with their properties, as well as those of the solvent and solute. It has been a formidable task to reach sets of ion properties that yield the underlying properties of recurring Hofmeister ion trends. In early attempts, Collins and Washabaugh[55] found 30 characteristics of salt solutions, showing the Hofmeister trends in polarizability, ionic size, and hydration-free energy. However, finding the well-characterized Hofmeister ion parameters is still a challenge. Leontidis proposed that a combination of hydrophobicity[56], size, shape, and ionic

charge distribution leads to the Hofmeister series. To suggest a basic SIE series that is solvent-independent, Mazzini and Craig[57] showed consistent SIE patterns for ions in a range of solvents. The study of intermolecular forces driving SIEs provides the connection between the observed ion-specific effects and basic ion characteristics.[58]

Polarizability has been found to correlate with experimental parameters of observed specific ion effects. Correlations are observed between ion polarizability, ionic radii, and ion ordering within the Hofmeister series. In order to explain the Hofmeister series in relation to electron density, especially for monovalent and monoatomic ions, Parsons and Ninham estimated a variety of ion characteristics, including Gaussian radii[59]. However, these correlations are limited when applied to polyatomic ions, including sulfate, carbonate, acetate, and others, since the Gaussian radius calculation gives inconsistencies when non-interacting groups are included. Differentiation based on localized charge may be necessary to unravel trends, as observed with anions where strong interactions are dominated by electrostatic intensity rather than polarizability. One such instance is the different behavior of ClO_3^- and IO_3^- ions, where the surface charge density affects the more "kosmotropic" character of IO_3^- ions even if they are highly polarizable[60].

Collin's Law of Matching Water Affinities emphasizes the importance of ion size for polarizability and ion pairing, which has a connection with the Hofmeister series [41,42,59]. Weak orientation-dependent bindings are shown by the delocalized and polarizable electron density of large symmetrical ions like I^-, whereas strong orientational interactions are exhibited by small ions with high charge density like F^-. Large ions can be partially dissolved more quickly because they tend to have weaker solvation shells[61]. Ion size is the key factor in determining the non-Hofmeister SIEs which affects both porous nature of ion and its ability to bind to macrocyclic receptors [62,63,64] The shape of ion plays a significant role that leads to coexisting moieties, multiple binding sites, or anisotropic charge densities. The location of charge in a polyatomic ion is crucial; the highest density of charges on a distal moiety determines the strength of the interaction, whereas internal density may result in shielding, as observed in the case with tetraphenyl ions and tertiary ammonium cations, where charge independence is indicated by higher-order interactions governing their effects [33, 65, 66]. In order to measure specific Ion Effects (SIEs), Gregory *et a*l. have recently developed a radial charge density variable ("sho"), which is site-specific This parameter,

which comes from Coulomb's Law, approximates the electrostatic interaction between an ion and its solvent environment irrespective of the system[65].

It pertains to basic features of aqueous electrolytes for anions, such as hydration energies and viscosity B coefficients, and to assortment of phenomena, such as non-aqueous chemical processes, colloidal stability, and the activities of enzymes. The "sho" parameter is more relevant to anions than to cations, indicating that even if anions are bigger and more polarizable, electrostatic interactions are still more important in aqueous solutions for anions. When extra co-solutes are present, cation-induced SIEs become more susceptible to non-Coulombic events due to their more prominent competitive behavior between the components of ion-solvent interactions.

1.2. Ion Specific behaviour at the Interface between air and water

The study of ions at the vapor-liquid (air-water) interface is a subject of fundamental interest, particularly the properties of ions at such an interface in the context of Specific Ion Effects (SIEs).[67-69]As seen in Figure 2, the interface makes ion specificity more challenging. The interface between air and water is considered the easiest to study and an example of hydrophobic surfaces, regardless of their complexity. Although the significance of interfaces has long been recognized, the femto-to-picosecond time scale of molecular motions makes classic experimental methods like STM and AFM inadequate for studying liquid interfaces.[71-73] Neutron reflectivity and X-ray spectroscopy can be effective for some applications but show limitations when applied to bathed aqueous interfaces.[74-78] However, with the help of sum frequency generation (SFG) and optical second harmonic generation (SHG) the selective exploration of liquid interfaces becomes possible.[79] These methods enable in-situ investigation of any interface that is approachable by light, resulting in specified output and sub-mono layer sensitivity that sheds light on molecular interactions at liquid interfaces. As the dielectric function is decreased locally in comparison to the bulk gives rise to a reduction in the density of water, and has an impact on charge screening and ion hydration.

These parameters with the combination of others used to determine the behavior of ions at surfaces. The ordering of the Hofmeister series is essentially caused by the behavior of ions at the surface, as demonstrated by surface-specific measurements like SFG and molecular dynamics simulations.

Ions that are responsible for the precipitation of proteins are more hydrated and have less ability to interact with the surfaces.

It is noteworthy that the majority of aqueous solutions found in real life have many ionic species. For example, seawater contains few organic ions and a large number of highly saturated inorganic ions, such as Cl^-, Na^+, SO_4^{2-}, and Mg^{2+}. It is believed that such small organic species are absorbed at the surface of the sea, and influence the physical and chemical processes such as the production of algal blooms and sea-spray aerosols.[80,81] Consequently, many studies have focused on comprehending the mechanics of ion interactions at different surfaces.

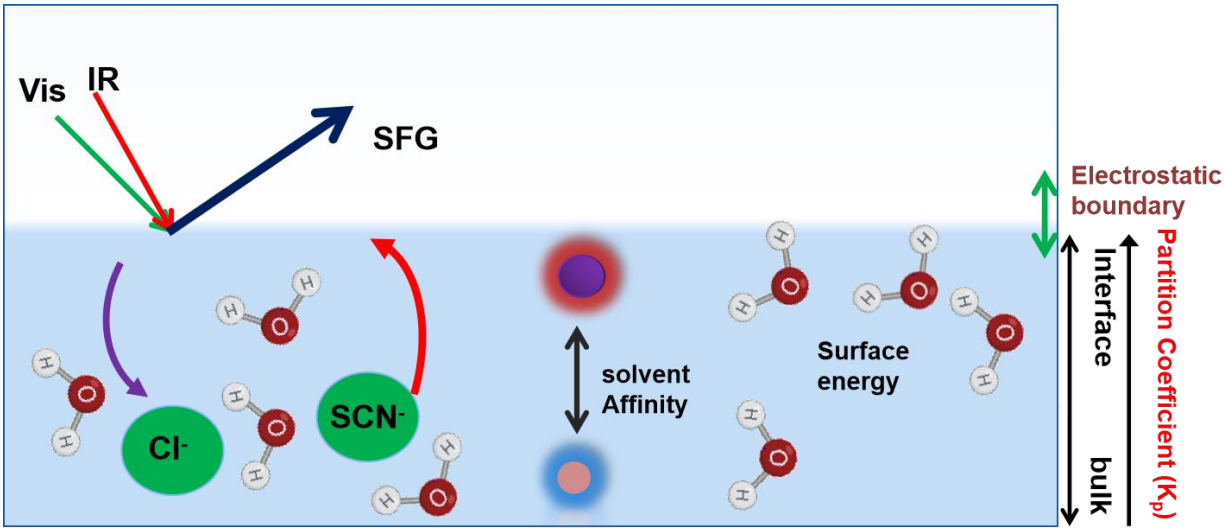

Figure 2: Techniques, ion specification and theories used to understand the effect of Hofmeister ion at air/aqueous interface: SFG (nonlinear laser spectroscopy) used to study surface activity of ion, indicating strongly hydrated anions depleted from interface and remain in bulk while weakly hydrated attracted toward the interface. Theories such as Solvent affinity, surface energy and counterion effect have been proposed to elucidate SIEs at air/water interface.

1.3. Ion specific water macromolecules interactions at Air/Aqueous interface

The specific Ion Effects also exist at the interface between macromolecules and water. However detailed mechanism is still a mystery. Polyvinylpyrolidine (PVP)/water interface was used as a model system by Kailash C. Jena and colleagues to demonstrate the Hofmeister effect at the water/polymer interface by using SFG. It was observed that the water molecules' ordering and SSP

polarized spectra at the interface follow the same ordering as the Hofmeister series, resulting from direct interactions between ions and macromolecules[82].

Interestingly, no structural changes in the backbone of the macromolecule occur due to the presence of ions. However, the CH-stretch region in PPP polarized SFG spectra shows that the ions influence the angle of orientation of the pendant vinyl chain of CH_2-groups, following the Hofmeister series: $SO_4^{2-} > Cl^- > NO_3^- > Br^- > ClO_4^- > SCN^-$. An important finding is the minimum orientation angle of CH_2-groups, which indicates a considerable rearranging in PVP vinyl chains when chaotropic anions SCN^- and ClO_4^- are present. This sequencing is related to the influence of individual ions on the water-macromolecule interaction at the interface between the polymer, water, and air. In addition, the spectral changes in the OH-stretch area (shown in Figure 3), when chaotropic anions are present in the PPP polarization, provide depth. The reason for these changes is that the backbone -CH and -CH_2 moieties of PVP macromolecules interact less strongly with interfacial water molecules. The relative tendency of anions to adsorb towards the air/aqueous boundary highlights the ion-specific modification of the hydrating water-macromolecule interactions. The results of this study offer insight into the real-world presence and cooperative engagement of ion-specific water-macromolecule interactions.

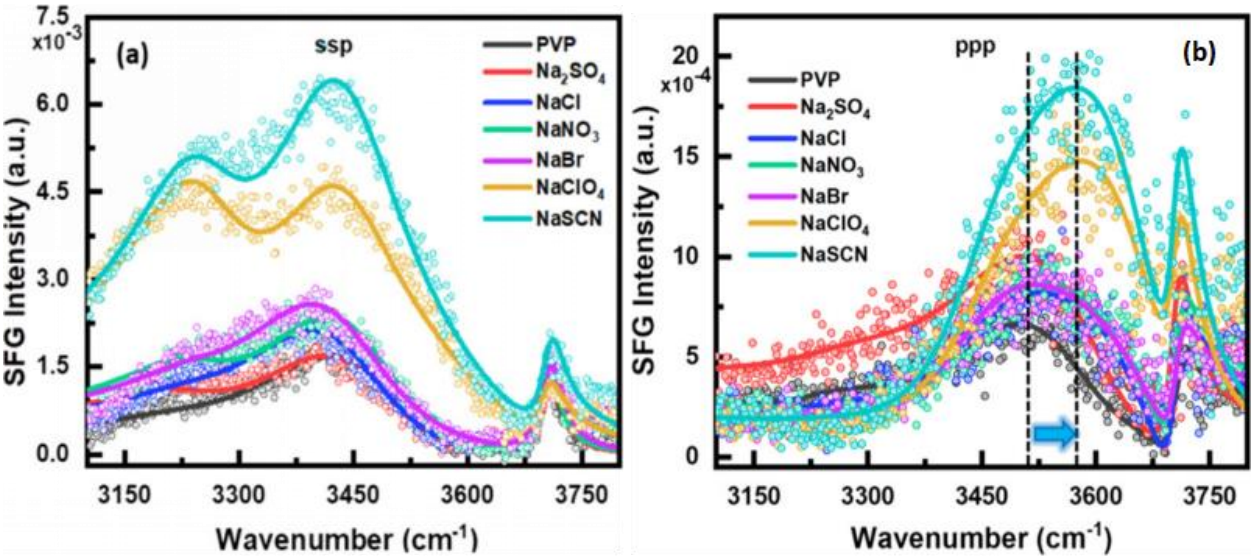

Figure 3: (a). Sum frequency generation spectra (ssp-SFG) (b) ppp-SFG spectra. Both sets of spectra were obtained at air/PVP/water interface in presence of aqueous 1 M sodium salts (Na_2SO_4, NaCl, $NaNO_3$, NaBr, $NaClO_4$ & NaSCN) solution demonstrating distinctive variation in OH

region intensity specific for each ion. Points in spectra show experimental data while solid lines represent the fitting curves based on Lorentzian fit. (adopted from Ref 82).

1.4. Direct Ion-binding to Macromolecules

The physicochemical characteristics of colloidal and biological systems, including the association of macromolecule and activity of protein, are strongly influenced by the salt ion content of the surrounding water solution. This effect depends not only on the valency and amount of salt but also on the ion's solvation properties. Nevertheless, the description of the Hofmeister effects is incomplete due to the absence of a distinct molecular-level representation.

According to recent discoveries, ion binding to macromolecules rather than water structuring effects is the source of many ion-specific effects. It is essential to investigate ion-macromolecular binding processes in extensive detail. The following are some of the molecular forces at work: [83-85]

1. The neutralization of counter-ion distribution occurs due to Coulombic interactions at the outside charged molecular surfaces.

2. Regardless of polarity, all atoms are subject to short-term dispersion or London-type interactions, which are only weakly eliminated by salt. The roughly proportionate link between an electron cloud volume and the high-frequency polarizability of a particular species results in ion-specific effects. By integrating continuous electrostatics with dispersion interactions, researchers have investigated biological and colloidal systems using this idea.[86, 87]

3. Massive, polarizable ions like thiocyanate and iodide may be attracted to weakly solvated surface groups like the air and water interface. In contrast, the reaction field in classical electrostatics describes the repulsion experienced by tiny, highly dissolved ions.[88,89]

4. The concept of "ion pairing," which dates back to the early 1900s, describes the possibility of a short-lived, net-neutral, zwitterionic species forming when a cation and an anion interact strongly. Ion-specific pairing occurs when distinct charged groups on the surface and free ions couple with differing strengths. For example, ion binding to negatively charged protein surfaces has shown that preferential binding to carboxylic groups is the primary cause of sodium's selectivity over potassium at the protein surface.[90,91]

Iodide and fluoride anions were distributed across a spherical macromolecule with and without discretely charged patches, employing detailed solvent molecular dynamics modeling.[86-92] Iodide,

which is less weakly hydrated, was slightly pulled by the surface of the uncharged macromolecule, but fluoride, which is robustly hydrated, was repelled. Both anions were drawn to the charged nanosphere differently: (1) A tiny ion called fluoride overcame resistance from the hydrophobic nucleus of specific anion-cation interactions. (2) A more delocalized, hydrophobic affinity led to the formation of ion pairs with the large ion iodide.

Overall, the MD simulation investigations show that hydrophobic and hydrophilic relationships impact particular ion bindings the most, while dispersion interactions have little to no effect. Iodide binding was favored when positively charged groups were positioned below the surface, but fluoride binding was favored when the surface charge density was increased. Therefore, neighborhood interactions control the particular anion interaction. Although the generalized coarse-grained method is qualitatively consistent with molecular dynamics simulations of short peptides and bulk electrolyte data, the specific characteristics of fundamental macromolecules in biological systems are expected to affect the quantitative binding of tiny ions.

1.5. Hofmeister effect on the amide-based macromolecules

As the previous section aimed to demonstrate, specific ion effects in aqueous solutions and at the air-water interface, the parameter introduced and utilized to explain the specific ion effects is system specific. What works for bulk aqueous solutions, does not work for protein surfaces. As such, a more system-based approach should be adapted to predict the ion's influence on a particular set of molecules, such as proteins. In this part of the thesis, a summary of the studies focusing on understanding the SIEs on amide-based macromolecules is prepared.

1.5.1. Understanding the anionic effect-Molecular level mechanisms

Model systems using polymer exhibiting a lower critical solution temperature (LCST, the temperature at which a polymer becomes insoluble in solvent, undergoing a phase transition from a soluble to insoluble state) have been employed to investigate how various salts impact the stability of biological macromolecules. These polymers consisting of hydrophilic groups, predominantly amide group, along with hydrophobic group, can promote macromolecule solvation at low temperature by forming hydrogen bonding with water. On the other hand, as temperature rises, the hydrophilic interactions with water counteract the hydrophobic interactions, causing the polymer chains to collapse and the solution to phase separate. This phase transition temperature is

strongly influenced by dissolved electrolytes, and it has been suggested that ion-specific interactions with the macromolecule's hydrophobic and amide groups are responsible for this impact. In polymers like poly(N,N-diethyl acetamide) or poly(N,N-isopropyl acrylamide) (PNIPAM), experiments with sodium salts encompassing the anionic Hofmeister series demonstrated the ion selectivity of the LCST. Remarkably, influence of salts on these macromolecular systems' LCST reflects their effect on the stability of the protein, frequently in the form of a Hofmeister series. [93,94s]

PNIPAM undergoes a phase transition in aqueous solution typically around 32 ℃, resulting in a change in configuration from random coil to globule because of hydrophobic collapse at this temperature. This phenomenon closely resembles cold denaturation behavior observed in the case of proteins.[95] Moreover, the chemical structure of PNIPAM (as shown in the Figure 5a) is composed of the hydrophilic amide group in the side chain, which mimics the hydrophilic peptide group and hydrophobic backbone groups (the isopropyl group in the side chain) similar to the hydrophobic side chain of natural proteins. This presence of these similar groups with varying chemical environments and degrees of hydrophobicity makes PNIPAM-type polymers an ideal model for investigating how the polarity of polymer groups affects their preferential interaction with ions.

Zhang and coworkers in 2005 performed a comprehensive study to probe the effect of 11 different sodium salts on the phase transition temperature of PNIPAM. They employed their newly-developed microfluidics/dark field microscopy to get unprecedented precision in data collection[96]. The study revealed that PNIPAM exhibited a direct Hofmeister series for anions. Specifically, the most strongly hydrated anions proved to be most effective at salting out, causing a linear decrease in LCST versus salt concentration, in contrast to weakly hydrated anions, which were comparatively less effective and introduced a salting-in component in the LCST curve, which manifested as a non-linearity at low concentrations.

An empirical model to fit the data quantitatively was introduced:

$$T = T_0 + c[M] + \frac{B_{max}.K_A\,[M]}{1 + K_A[M]} \qquad (1)$$

Here, the measured LCST (T) of PNIPAM is related to the LCST in the absence of salt (T_0) and molar salt concentration ([M]) with *c* as a coefficient in units of ℃/M and the last term is derived from a Langmuir-type binding isotherm. Likewise, K_A represents the association equilibrium

constant (apparent) and denotes the maximum change in LCST because of ions binding at saturation. LCST curves for all the examined salts could be fit using equation 1, but in the case of strongly hydrated anions, the nonlinear term in the above equation is zero because the curve is linear. Subsequently, they compiled and presented all the relevant parameters tailored to each salt based on the fitting process. Then, the authors proposed a molecular-level mechanism composed of three main parts, which give ion-specific results. This proposed mechanism was based on their comparative analysis of fit parameters used to describe various physicochemical characteristics of the ions. Notably, negative values of co-efficient *c* responsible for the salting-out process demonstrated a strong correlation with the entropy of hydration in the case of strongly hydrated anions and an increment in surface tension for weakly hydrated anions. This interpretation led to the conclusion that these two classes of anions should have a separate mechanism for the salting-out process. For weakly hydrated anions, the salting-out effect is attributed to the destabilization of the polymer's hydrophobic hydration caused by increased surface tension of water.

Conversely, for strongly hydrated anions, this mechanism is explained on the basis of the polarization of water molecules around the polymer. This polarization, in turn, weakens the hydrogen bonding among water molecules and amide groups on the side chain, leading to a salting-out effect. The third mechanism they proposed was bonding the weakly hydrated anion at specific sites on the polymer backbone. This binding thermodynamically stabilizes the polymer in soluble form as shown by Langmuir type binding isotherm relation, shown in the last term of equation 1. This suggests that saturable binding may occur in the system. Furthermore, the B_{max} term magnitudes for weakly hydrated anions aligned with the reported order (ClO_4^-, SCN^-, Br^-, NO_3^-, Cl^-) for polyacrylamide gels[97], poly(*N*-vinylpyrrolidone)[98] and small peptides[99] in previous studies. A similar study was conducted by Cho *et al*. in 2008 to investigate the solution phase behavior of two types of elastin-like polypeptides (ELP) with 11 sodium salts present.[100] Their main aim was to determine whether a distinct mechanism proposed by Zhang et al. for PNIPAM held for polypeptide, a different thermoresponsive polymer, may serve as a more accurate approximation to natural proteins. ELPs exhibit a unique phase change at LCST points, typical of polypeptide composition and molecular weight.[101] It should be noted that, however, neither Zhang and coworkers nor Cho et al. were able to pinpoint the exact position of preferential interaction site for weakly hydrated anions beyond the anticipated localization around the amide or peptide group. Subsequent studies, however, more rigorously determined the binding site of these interactions.

A 600-residue elastin like polypeptide having a sequence $(VPGVG)_{120}$ (Figure 5d &f) show the structure) was studied by Rembert *et a1*[102] which correspond to one of the polymer study by Cho *et al.* The study focused on the sodium salt of chloride, iodide, thiocyanate and sulfate anions. To describe the behavior of the ions at various study levels and offer reliable support for their suggested model, they integrated LCST observations with quantitative ^{1}H-NMR spectroscopy and molecular dynamics (MD) simulations. The results of their thermodynamic analysis were consistent with those of Cho *et a*l., and the LCST curves were fitted to a restructured, identical version of Equation 1:

$$\Delta T = -c[M] + \frac{B_{max}\,[M]}{K_D + [M]} \qquad (2)$$

Here, K_D is the dissociation equilibrium constant for ion binding, and ΔT is the shift in LCST when compared to the polypeptide in the absence of salt cosolutes. In other words, a stronger, "tighter" binding is indicated by a lower K_D value.

The identical LCST behaviour previously established by Cho *et al.* was successfully replicated (demonstrated in Figure 4 (left panel)). The critical aspect of this study was the use of quantitative, externally-referenced ^{1}H-NMR spectroscopy to observe change in the behavior of all protons on the polymer as a function of added salt.[100] The same set of salts were essentially used for NMR titration, which were conducted with samples in NMR tubes equipped with an extra coaxial insert tube that held the chemical shift reference standard sodium 2,2-dimethyl-2-silapentane-5-sulfonate (DSS), used for external referencing without coming into contact with the sample solution chemically. The measurements were made at 5 °C in order to stay below the mixtures' LCST. By classifying each proton chemical shift according to its local chemical environment on the polymer, they were all recorded and examined. By classifying each proton chemical shift according to its local chemical environment on the polymer, they were all recorded and examined. Protons associated with hydrophobic valine side-chains as well as the water protons for all salts were among those that showed chemical changes that decreased linearly with increased salt. However, notably protons at the α-position on the backbone (that is, on methylene groups next to amide N atoms or carbonyl groups) showed the nonlinear chemical shift curve while interacting with salts of weakly hydrated anions. Preferential interaction at these locations is the origin of the molecular level thermodynamic effect, as demonstrated by the shape of the curves, which closely followed

the trend exhibited by similar salts on the LCST's of the polymer. After that, the chemical shift curves could be fitted to a mathematical form given below that was very close to Equation 2:

$$\Delta\delta = -c[M] + \frac{\Delta\delta_{max}\,[M]}{K_D + [M]} \qquad (3)$$

where a saturable and deshielding (chemical shift increasing) interactions with the weakly-hydrated anions is responsible for the change in chemical shift (Δδ). As demonstrated by the binding of SCN^- to α-position (as shown on the ELP structure), the dissociation constant (K_D) for these interactions was determined to be as low as 50 mM. in Figure 4(b).

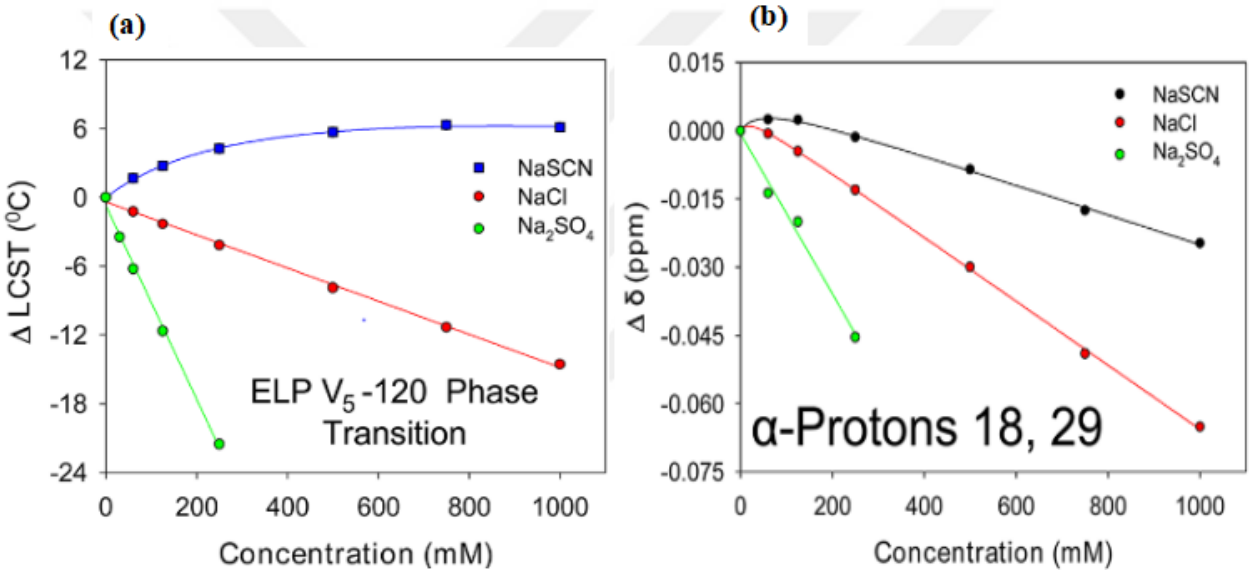

Figure 4: (a). The lower critical solution temperature (LCST) of ELP V_5-120 as a function of three sodium salts (NaSCN, NaCl, and Na_2SO_4). (b). The chemical shift values from ^{1}H-NMR for alpha Proton of ELP V_5-120 as function of sodium salt (same as for LCST). It can be seen from right figure that increase in chemical shift value for α-protons at low salt concentration depicts the binding in case of NaSCN.[100,101]

Similar thermodynamic and spectroscopic experiments of poly(*N*,*N*-diethyl acrylamide) (PDEA), an ethylated derivative of PNIPAM with a structure comparable to PNIPAM but without an N-H group in its side chain, were carried out by Cremer and colleagues.[103,104] Their findings further decentralized the significance of the N-H moiety in the kinetics of anion binding and largely accorded with the observations of Rembert *et al*.

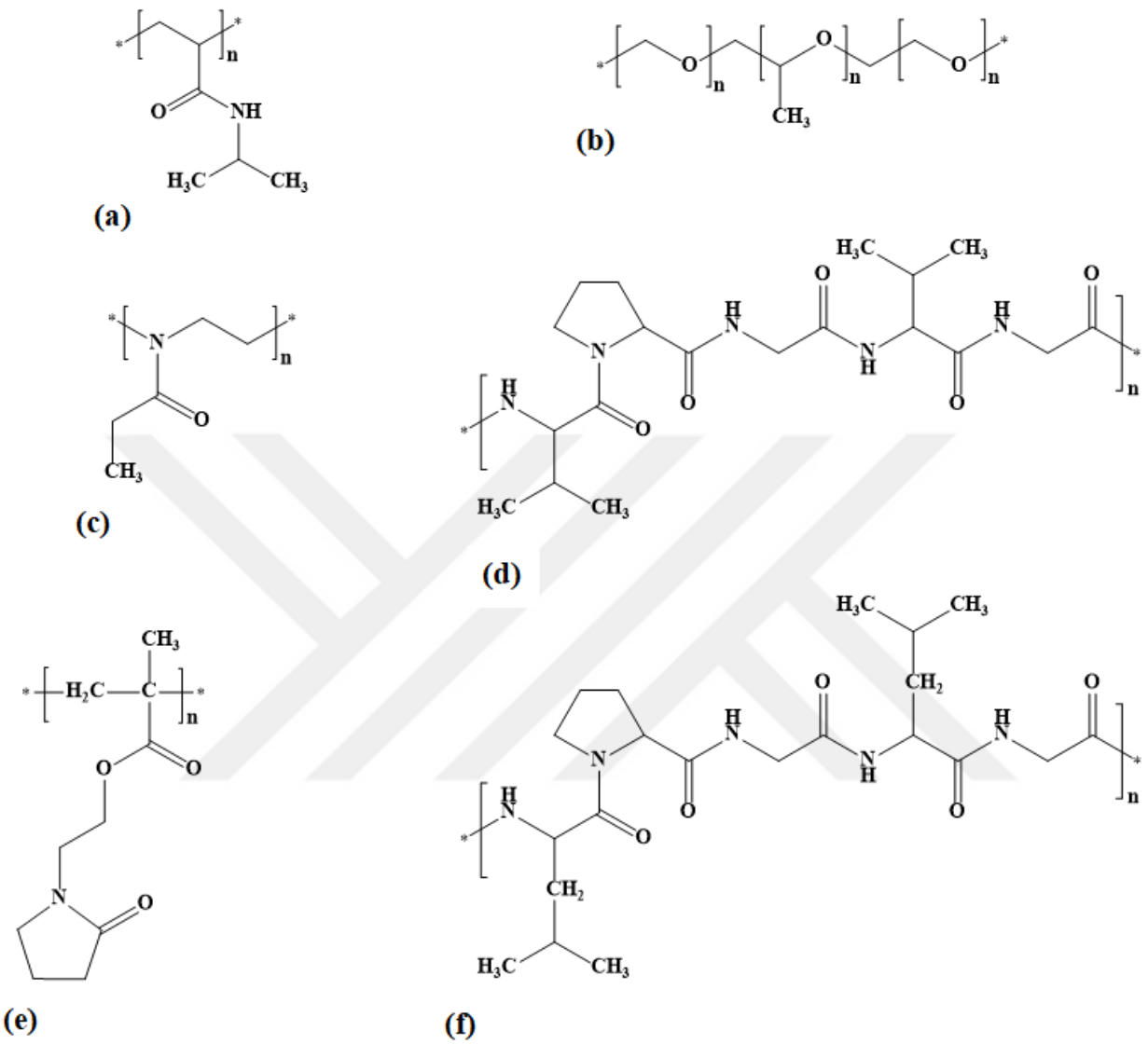

Figure 5: Chemical structures of amide based macromolecules for which Hofmeister effect is known (a): poly(*N*-isopropyl acrylamide) (PNIPAM) (b):Pluronic polymers (c): poly(2-ethyl-2-oxazoline) (d): 600-residue elastic like polypeptide (e): poly[*N*-(2-methacryloyloxyethyl) pyrolidone (f): ELP V_5-120.

1.5.2. Understanding the Cationic effect-Molecular level mechanism

In the Hofmeister effect literature[105-108], anions have often received greater attention compared to cations. Studies generally agree that anions predominates over the influence of cations, with reasons based on their greater size and stronger polarizability. The explanation for this asymmetry

is that water has a high electronegativity which makes it more likely to accept electron transfer from anions during hydration but less likely to give charge to cation.[109-112] spectroscopic studies on interaction of with amides have been performed recently and the findings show that strongly hydrated cations exhibit a weak but observable affinity for amide carbonyl. In their 2013 study Okur *et al.* examined butyramide in metal chloride salts solutions and found that the presence of Ca^{2+}, Mg^{2+}, and Li^{+} ions caused a blue shift in carbonyl stretching mode. It was demonstrated that with an increase in salt concentration, cation-bound salt concentration increases as well with Ca^{2+} showing the highest binding. Later, FTIR and ab initio theoretical investigations corroborated cations partitioning at air/solution interface in case of direct Hofmeister series was validated by VSFS measurements.[113,114]

A comprehensive study was reported by Bruce *et al.* in 2020 to investigate the effect of cations on neutral macromolecules (PNIPAM) using nine metal salts.[115] Despite the anticipation of salting out effect for all salts on the polymer, cations such as Mg^{2+}, Ca^{2+}, Sr^{2+}, Li^{+} -which are strongly hydrated-demonstrated a partial salting-in effect, contrary to expectation based on anionic behaviour. The research presented an empirical model with both linear and quadratic terms for the LCST curves. Accumulation of ions around amide oxygen and nitrogen were demonstrated by MD simulations, suggesting the occurrence of solvent shared ion pairs especially with strongly hydrated cations.

Very recently in our lab (Okur research group) interactions of weakly hydrated cation (tetraalkylammonium) with model polymer PNIPAM were investigated by using NMR and ATR-FTIR spectroscopy. It was found out that these cations significantly binds to macromolecules producing salting-in effect that are similar to those of weakly hydrated anions. The direct cationic Hofmeister series on neutral macromolecules revealed by these investigations highlights the subtle cationic contribution that is masked by greater effects in a variety of systems.

1.6. Specific ion effect as a function of size and charge of macromolecules

In the preceding sections, we discussed the impact of ions on both small molecules and macromolecules, exploring how ions can influence their properties. Here in this section, our focus will be on examining how specific ion effect is influenced by the charge and size of molecules.

For instance, interaction of Hofmeister ions with small molecules such as trigylcine (chemical structure given in Figures 6 a and b) has been studied by Paterova *et al.* by NMR spectroscopy and Molecular Dynamics (MD) simulations [116] . They found that uncapping the N-terminus (RNH_3 to RNH_2^+) induced a reversal in the ordering of anions. Specifically, terminated triglycine showed no significant binding with SO_4^{2-}, Cl^-, and Br^-, while I^- and SCN^- exhibited weak binding (K_D >1000 mM). The apparent dissociation constants (K_D in mM) for non-terminated triglycine followed the order: SO_4^{2-} (70 ± 30) < Cl^- (290 ± 240) < Br^- (890 ± 560) < I^- (>1000) < SCN^- (>1000). This highlights the significant influence of cosolute presence on chemical and physical properties related to SIEs. The findings suggest potential similarities between the impact of cosolute and pH changes on these properties.

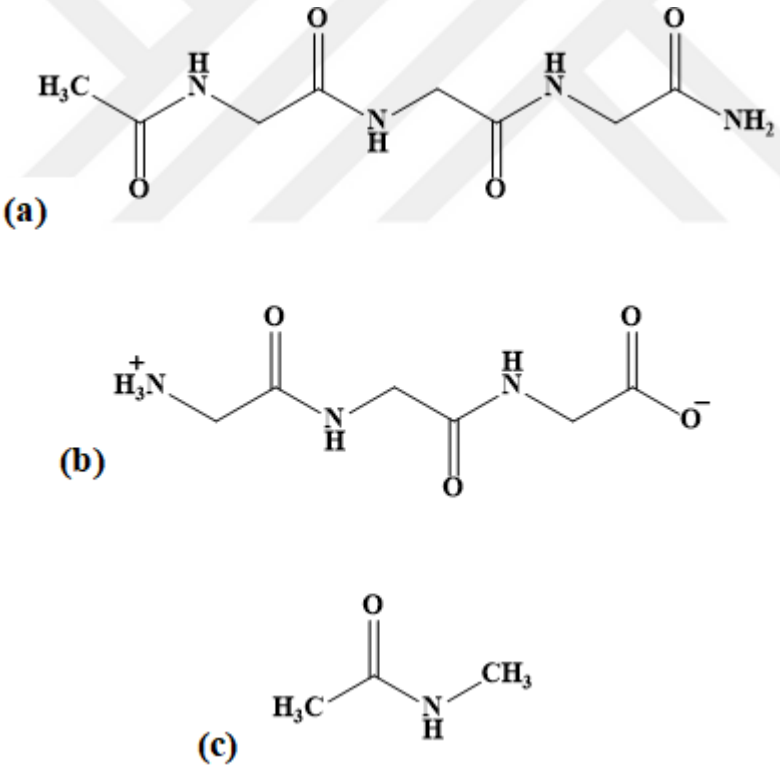

Figure 6: Small molecules for which Hofmeister effect is known (a): capped triglycine (b): uncapped triglycine (c): N-methylacetamide. Okur *et al*., who examined the Hofmeister effects on protein surfaces, reached to similar conclusions [116].

Similarly, Bradley A. Rogers and coworkers[41] studied the SIE for polyethylene glycol oligomer and polymers of varying molecular weights. An apparent paradox arises in aqueous solutions where weakly hydrated anions facilitate the solubilization of hydrophobic macromolecules, while small molecules with identical chemical components precipitate in the presence of these ions. This contradiction is clarified through a systematic investigation of the interactions between NaSCN and oligomers and polymers with variable molecular weights of polyethylene oxide. Spectroscopic and computational analyses reveal the preferential accumulation of SCN^- near the surface of polymers while being excluded from monomers. This behavior arises from the preference of SCN^- to bind to the center of macromolecular chains, disrupting the local water hydrogen-bonding network. These findings imply a connection between ion-specific effects and theories explaining how the modulation of hydrophobic hydration is influenced by the size and shape of a hydrophobic entity.

Now, in this study, we are specifically focusing on exploring the influence of ions on amide-based oligomers – these are molecules that are not as small as regular ones but not as big as macromolecules. These oligomers vary in size and charge. Our goal here is to figure out how ions interact with these oligomers of different sizes and charges. This research will help us understand more about how ions specifically impact these in-between-sized macromolecules.

1.7. Hofmeister ion and sugar-based Macromolecules

The molecular mechanisms by which the Hofmeister ions interact with polymers, poly-peptides, and proteins have been extensively investigated. It has been shown that direct binding to macromolecules or ion exclusion governs the observed series.[117] More complex ion behaviors are also demonstrated. These insights into Hofmeister ion interactions with amide-based polymers enabled the establishment of the molecular level detailed mechanistic picture of ion-macromolecule interactions. Surprisingly, the influence of Hofmeister ions on the other physiologically relevant macromolecules, the sugar-based ones, remains mainly unexplored. Sugar-based macromolecules, especially cellulose, hyaluronan, and the sugar-oligomers at the cell surface play important roles in biological systems and have a wide range of applications, such as cell signaling[118], tissue regeneration[119], and drug delivery[120].

We aim to explore the Hofmeister ion sugar-based neutral macromolecule interactions by focusing on hydroxypropylcellulose (HPC) as a model polymer (see Figure 7B for molecular structure). In this study, HPC with sodium salts of 8 anions (NaSCN, NaI, $NaNO_3$, $NaClO_4$ NaCl, Na_2SO_4, Na_2CO_3, NaH_2PO_4) were utilized to investigate the SIE on the phase transition temperature of HPC. To achieve a molecular picture of ion interactions ^{1}H-NMR spectroscopy was utilized.

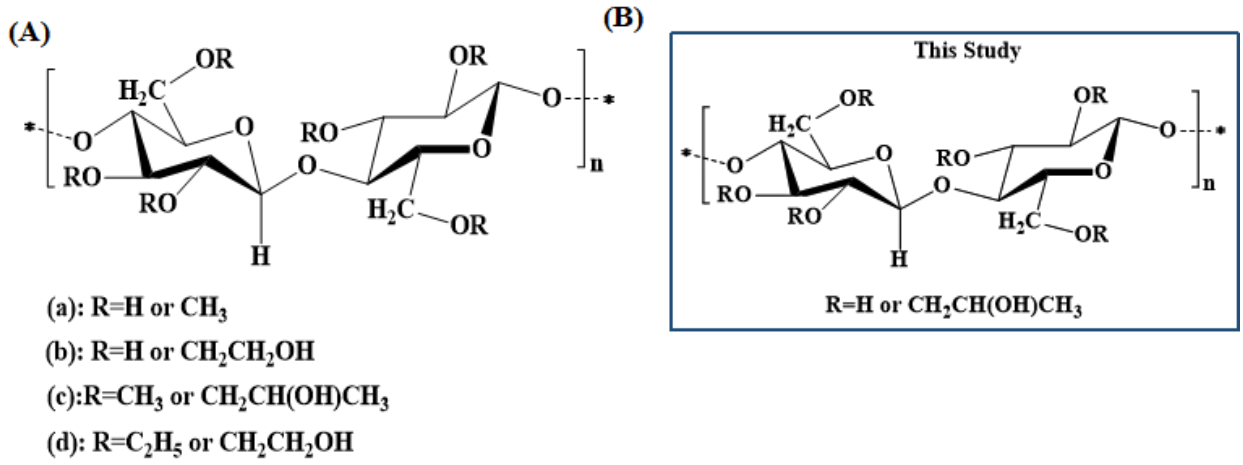

Figure 7: (A): Sugar based macromolecules that can be employed to study ion-sugars interactions in aqueous solution. (a): Methyl cellulose, (b): Ethyl cellulose, (c): Hydroxypropylmethyl cellulose, (d): Ethylhydroxyethyl cellulose, and (B): Cellulose derivative use in this study: Hydroxypropyl cellulose (HPC).

Chapter 2-Materials and Methods

2.1. Materials

2.1.1. Chemicals

N-isopropyl acrylamide (NIPAM) (Acros organics, 99%) which was recrystallized in benzene (Panreac, 99.5 %) and n-hexane (98%) mixture. The initiators ABCN (1,1´-Azobis (cyclohexanecarbonitrile)) (sigma Aldrich, 98%), and ACVA (4,4´,Azobis(4-cyanovaleric acid) (Sigma-Aldrich, 98%) were used after recrystallization in methanol (99.8%). Isopropyl alcohol (Carlo Erba, 99.9 %) Dimethyl foramide (DMF) (sigma Aldrich, 99%) used as solvent. RAFT agent, 1,3,5-Trioxane (Reference for NMR), Dichloromethane (DCM) (Carlo Erba, 99.9%).

2.1.2. Salts

Sodium chloride (Sigma Aldrich, 99.99 % purity), sodium sulfate (Sigma Aldrich, 99.0 % purity), Sodium thiocyanate (Sigma Aldrich, 99.99 % purity), sodium iodide (Merck, ACS reagent), sodium phosphate dibasic (Sigma Aldrich, 99.5 % purity), sodium perchlorate hydrate (Sigma Aldrich, 99.99 % purity), sodium nitrate (Sigma Aldrich), sodium carbonate (Sigma Aldrich), ultrapure water (millipore Nanopure system, 18.2 MΩ cm), D_2O (Eurisotop 99.90 %) were employed without further purification. All the stock salt solutions were prepared with gravimetric method using 10 ml volumetric flasks with 18.2 MΩ deionized water or D_2O. The Na_2SO_4 solution was prepared up to 0.8 M due to its lower solubility. The remaining salt stock solutions were each prepared up to 1 M.

2.1.3. Oligomers and Sugars

All the synthesized oligomers and commercially available sugar-based polymer (hydroxypropyl cellulose) were subjected to lyophilization by using the method explained in subsequent section (2.2.3.2) prior to be utilized in any measurements.

PNIPAM oligomer with charged and neutral end groups were synthesized by method of free radical polymerization (explained in section (2.2.1) by using (4,4´,Azobis (4-cyanovaleric acid)

ACVA and 1,1′-Azobis (cyclohexane carbonitrile) **(**ABCN) initiators respectively having molecular weight of Mw = 2458 g/mol and 1372 g/mol determination by gel permeation chromatography.

Hydroxypropyl cellulose (HPC) was purchased from Sigma Aldrich with reported average molecular weight M_w ~ 80,000 g/mol and number average molecular weight Mn ~10,000. it was obtained as a powder with 20 mesh particle size.

2.2. Methods

2.2.1. Synthesis of Polymer by Free-radical polymerization

In a generic synthetic route 465.4 mg NIPAM and 13.2 mg 1,1′-azobis (cyclohexane carbonitrile) (0.0194:1 mole ratio) were dissolved in 20 ml isopropyl alcohol. Then, the reaction mixture was degassed by continuous nitrogen gas bubbling through the solution for about 30 min. The degassed reaction mixture was then transferred to a preheated (80 ℃) oil bath with continuous stirring. The reaction was allowed to run for at least a week. The reaction was stopped by cooling the reaction mixture to room temperature and by exposing it to ambient air. The resulting product was precipitated in diethyl ether three times. After precipitation, the solvent was evaporated, and the sample was dried to obtain the final product.

2.2.2. Synthesis of polymer by Raft polymerization

First of all, 633.55 mg NIPAM, 90.4 mg CTA, 15.69 mg ACVA and 15 mg 1,3,5-Trioxane were weighed and dissolved in 2 ml DMF in a glass vial equipped with a magnetic stirring bar. After dissolving 100 microliter samples (at time 0, t_0) were taken as a reference from the mixture before starting the reaction. The reaction mixture was degassed for 30 min by nitrogen purging. After degassing, the reaction mixture was transferred in a preheated oil bath (70 ℃) with constant stirring. Allowed the reaction to run for 8 h at constant stirring and heating rates. During the reaction, samples were taken after intervals of 30 min, 1 h, 2 h, 4 h, and 6 h to monitor the progress of the reaction. After 8 h, the polymerization was quenched by cooling the mixture to room temperature and exposing it to ambient air. As the reaction ended, a final (t_f) sample was taken for test measurements. Upon completion of the reaction, the mixture was precipitated in cold diethyl ether three times. (diethyl ether was kept in the fridge). To make the precipitation facile in

diethyl ether, as reaction stops, few drops of acetone were added. Then the reaction mixture was transferred in a centrifuge tube containing 40 ml of diethyl ether. As the reaction mixture was added to the diethyl ether, a precipitation starts and the solution turns to milky white color. Then the solid precipitates were collected by centrifugation. The samples were centrifuged using a temperature control centrifugation with 9000 rpm at 4 ºC for 20 min. After the first round of centrifugation the supernatant was transferred to a 50 ml falcon tube and the solid sample was collected. The collected sample was dissolved in DCM and precipitated in diethyl ether again and centrifuged using the same parameters. This process was repeated on the supernatant till no precipitation forms and the separated sample was dissolved in DCM due to its low boiling point and ease of evaporation. The sample was left in the fume hood by keeping its lid open for 30 min to evaporate DCM solvent. In the next step, the sample was dried using a desiccator, where the sample was placed in the desiccator by covering the opening with aluminum foil that contains small holes on it. The sample was the allowed to dry overnight. After drying, the sample was weighed for gravimetric yield calculation.

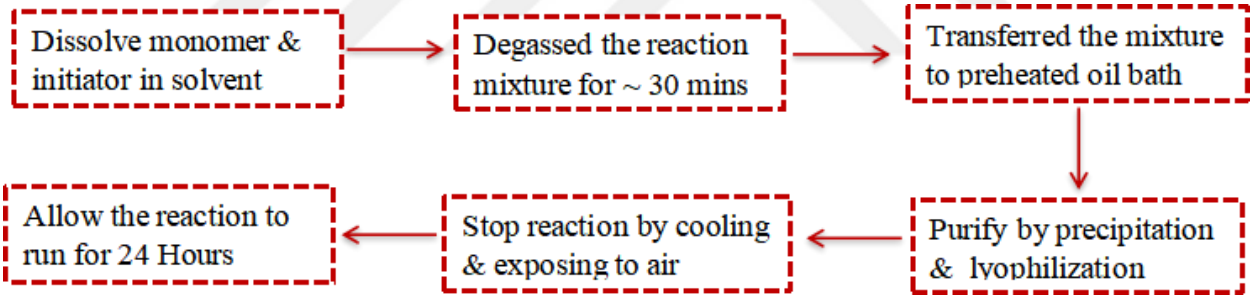

Figure 8: Flow chart demonstrating the main steps involved in the synthesis of the oligomer.

2.2.3. Purification of synthesized Oligomers

Both types of oligomers synthesized by RAFT or Radical polymerization were purified by using precipitation as well as lyophilization methods.

2.2.3.1. Precipitation

In case of RAFT polymerization since reaction was carried out in DMF (used as solvent), it was very hard to completely get rid of DMF. Thus, both precipitation and lyophilization methods were employed sequentially to achieve pure oligomers. For precipitation, diethyl ether as explained in section 2.2.2 was employed to sediment the polymer from the solution. However, by using diethyl

ether the entire polymer content of the sample could not be fully precipitated. Therefore, after centrifugation the left-over supernatant in diethyl ether which still contained a certain amount of oligomer was evaporated to remove solvent (diethyl ether) by rotary evaporator.

To further eliminate the DMF from the sample precipitation was also done in n-hexane. For precipitation, every 1 ml of sample was mixed with 14 ml of n-hexane yet no precipitate formation could be observed, there was complete phase separation instead of precipitation. On the other hand, the oligomers synthesized by radical polymers were precipitated using n-hexane. Since free radical reactions were performed in methanol and isopropyl alcohol medium, it was relatively straightforward to remove these solvents.

2.2.3.2. Lyophilization

Synthesized oligomers and sugar-based macromolecules utilized in this thesis were lyophilized to remove residual solvent and small molecule impurities. Stock aqueous solutions of samples (PNIPAM oligomer or HPC) were prepared by precisely weighing the desired amount of sample into a volumetric flask (generally 10 mg/ml final concentration) and by fully dissolving in deionized water to get the homogeneous mixture. Thorough homogenization was obtained by vortoxing the solution followed by keeping it in the refrigerator for at least 12 h. Intermittent mixing during refrigeration ensured complete dissolution. Subsequently, aliquots of needed volume depending on the final desired dry mass were meticulously transferred to the bottom of 2 ml Eppendorf tubes with the help of micropipette. The tubes were then sealed with punctured tube caps (lids with holes in it to enable evaporation of the solvent during desiccation).

Following this, sealed tubes were then subjected to freezing by using liquid nitrogen for a few minutes until all the mixture in the tubes were completely frozen. The frozen samples were then transferred to the desiccation chamber attached to a vacuum pump and subjected to complete drying under continuous vacuum for a minimum of 12 h. Subsequently, samples were removed from the desiccator, removed the punctured caps and closed with original caps and placed in the refrigerator for future use.

Whenever needed the lyophilized samples are dissolved in desired solutions within the Eppendorf tube by vortoxing.

2.3. Phase Transition Temperature Measurement

Phase transition temperature measurements were done by using melting point apparatus (Optimelt, Stanford Instrument, as shown in Figure 9) in triplicate by dissolving the sample in a relevant solution or solvent. The samples (100 microliters of polymer and oligomer solutions) were then loaded into capillary tubes, which were sealed on one end and open on the other with the help of syringes. The temperature of the tubes was ramped from 9 ℃ to 70 ℃ in the Optimelt apparatus at a ramp rate of 1℃ per min for all the samples. The ramp rate reduced the amount of time required to reach LCST and minimized the loss of water caused by any possible evaporation. The LCST was determined from the onset of scattering intensity relative to the flat and low-intensity baseline observed at colder temperatures.

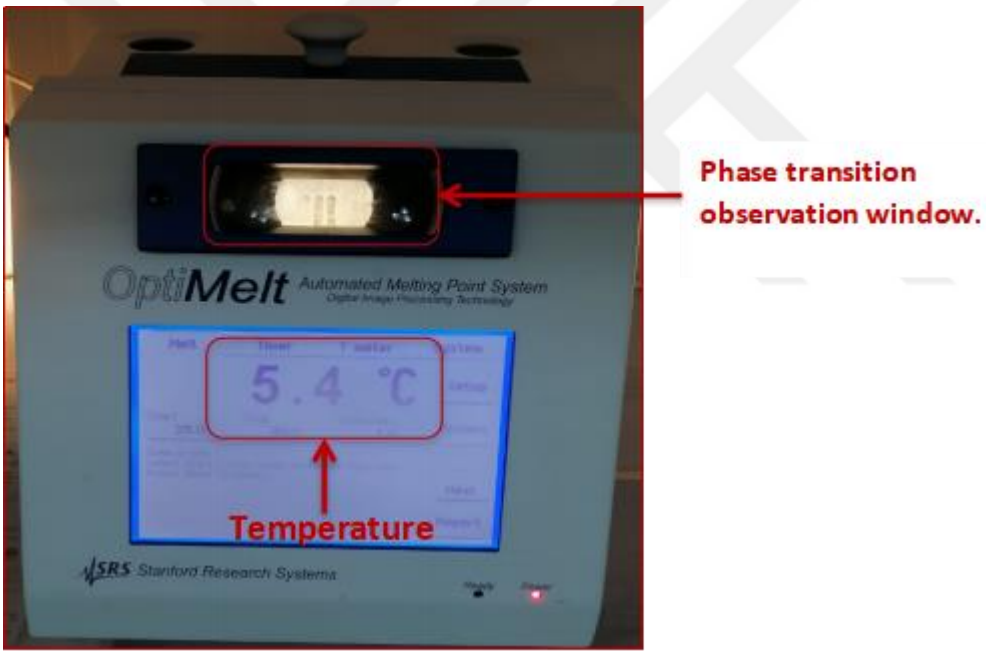

Figure 9: Optimelt instrument labeled with main visual parts the temperature screen. The phase transition window where real time phase transition of sample from clear to cloudy can be observed**.**

Below the phase transition temperature, solution of the sample (both oligomer and sugar-based macromolecules) were clear and homogeneous as can be seen in Figure 10 indicating low scattering intensities that generally remain constant with temperature. As the solution approaches the LCST, there is a noticeable and sudden increase in scattering accompanied by turbidity of solution which continues to increase until it reaches a maximum limit as can be seen in Figure 10

given below. The point where scattering starts increasing is referred to as cloud point or phase transition temperature or LCST.

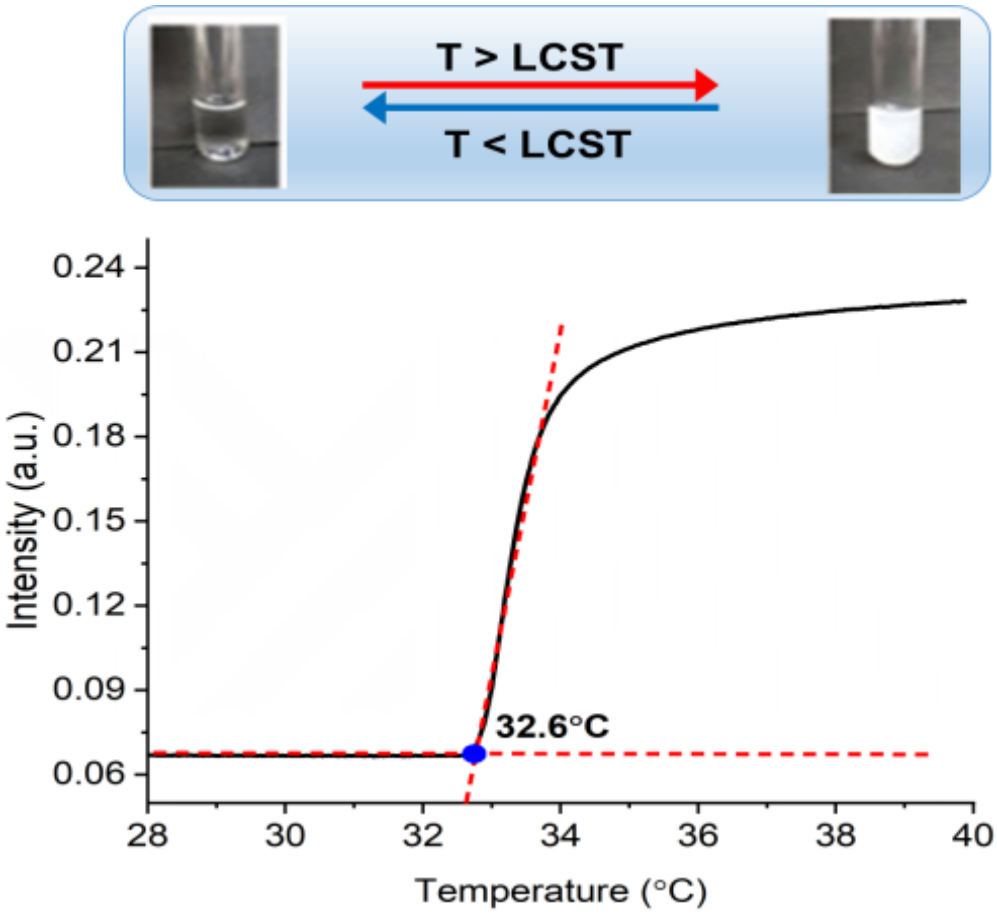

Figure 10: A depiction of representative scattering light intensity vs temperature plot synthesized PNIPAM oligomer in aqueous solution with tangent line drawn to the curve before and after phase transition temperature. The onset of phase transition temperature is highlighted as point of intersection marked with a blue circle (●). The top figure schematically illustrates the change in scattering intensity at T< LCST the solution is clear demonstrating no scattering whereas at T >LCST the solution is turbid showing high scattering intensity.

2.4. Nuclear Magnetic Resonance Spectroscopy Measurements

The ^{1}H-NMR measurements were performed on a Bruker AVANCE III 400 MHz spectrometer at room temperature. The samples were prepared in Deuterium oxide (D_2O) used as a solvent and analyzed SP Wilmad lab glass 5 mm thin-walled precision tubes equipped with SP Wilmad lab

glass coaxial insert for external chemical referencing to DSS (2,2-dimethyl-2-silapentane-5-sulfonate sodium salt). The reference (DSS) and locking agent (D_2O) with a volume of 150 µL. The insert was placed in a sample tube containing the 400 microliters of sample solution as shown in Figure 11. Both solutions were thus measured together simultaneously without direct physical or chemical contact. To match the spectrometer detector coil range, the sample and reference solution were prepared to have a height of around 5 cm in the both solution (sample and reference). The ^{1}H-NMR spectra were taken with Brukers's standard zg pulse sequence with acquisition time of 3.3 seconds and relaxation delay of 1 s. NMR spectra with an average of 32 scans were taken. Other standard procedures such as locking of solvent (Deuterium) signal, shimming and automatic tune matching are completed before every measurement.

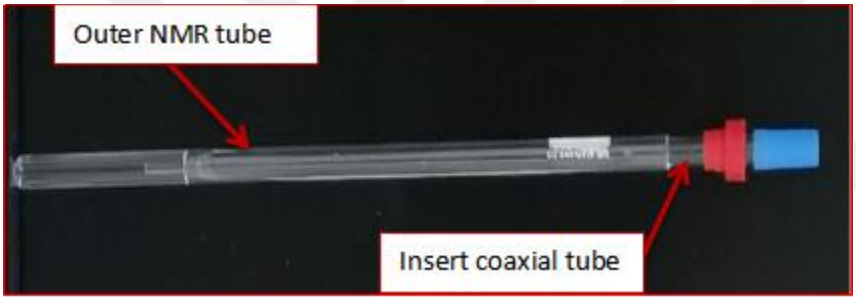

Figure 11: Demonstration of NMR tubes used to take NMR spectra. The inner one in Coaxial insert in which reference is placed to avoid interference between sample and reference while in outer one sample is kept.

As automated functions are applied on data in TopSpin (Brukers's standard NMR software which is used alongside NMR). Further data processing and manual correction were done by using Mnova from Mesterlab.com. Then processed data was subjected to phase correction and baseline correction before further analysis. The spectra after correction were subsequently referenced to the chemical shift of reference (DSS) main signal conventionally set at 0.0 ppm.

2.5. Molecular Weight Determination of oligomers

The molecular weight and polydispersity index (PDI) of the synthesized oligomers were determined by a gel permeation chromatography (GPC) method using Agilent 1260 infinity II Gel permeation chromatography (with THF as a solvent) as shown in Figure 12 equipped with auto-

samplers, multi-detectors (Agilent technologies) suite (MDS) containing combination of refractive index, light scattering and viscometer detectors and ZORBAX PSM 60 analytical (6.2× 250 mm, 5-Microns, Agilent technologies) column covering a broad molecular weight range of up to 100000 Da. The column and detectors were thermostated at 25 ºC. The samples were analyzed at a flow rate of 0.6 mL/min and injection volume was 20 µL. Both data collection and analysis were carried out using Agilent software.

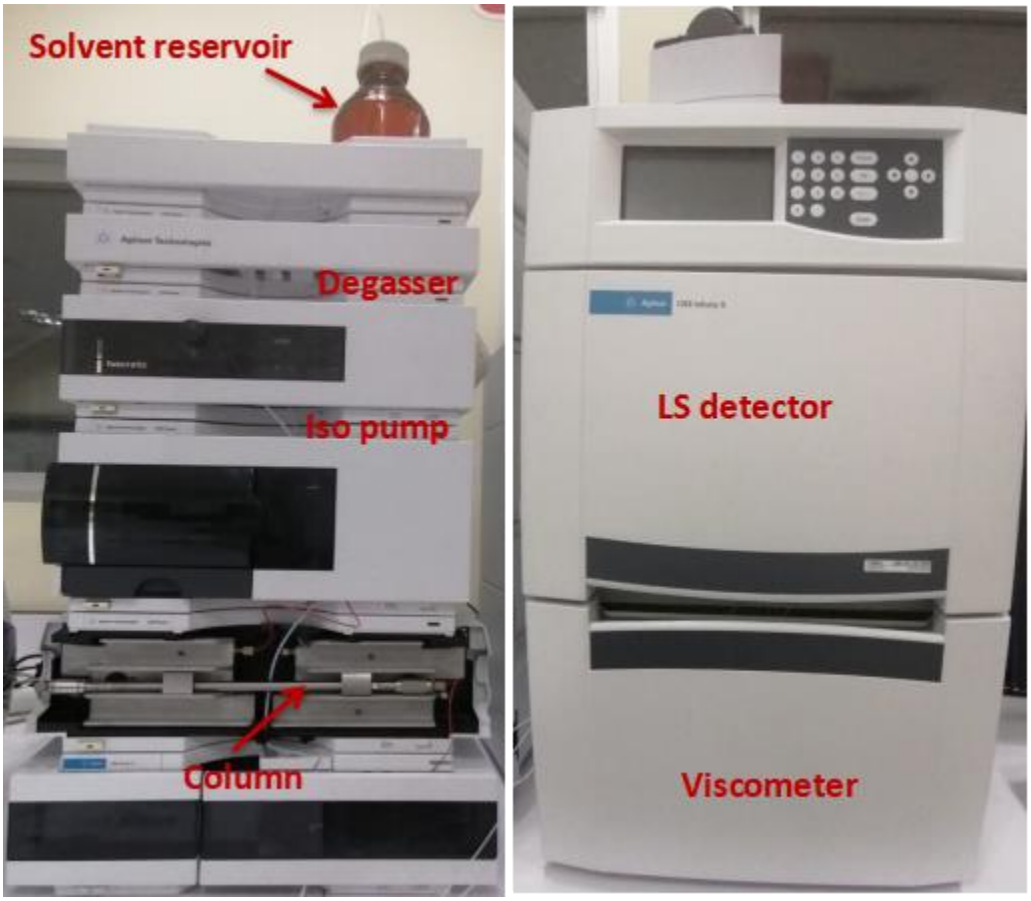

Figure 12: Agilent 1260 infinity II Gel permeation chromatography system.

Before measuring the molecular weight of oligomers, the samples were lyophilized in water to remove all the impurities. Then 10 mg of oligomers were taken and dissolved in eluent (THF) to make 1 ml solution in GPC vials. Subsequently, samples were placed in tray within the autosampler. Specifically, one of the vials in the tray was filled with THF designated as reference. At first eluent (THF) was run through the column to check the flow rate. Then samples were allowed to run and measurements were made. After sample measurement, reference samples of

known molecular weight for polystyrene (PS) and polymethylmethacrylate (PMMA) having narrow molecular weight distribution were analyzed. Note that both standards were not used at the same time, and the molecular weights were determined using each reference separately. Using Agilent software a calibration curve was generated as demonstrated in Figure 13 (red line with blue dots). Values from the unknown oligomer samples were then compared with the calibration graph to generate molecular weight and molecular weight averages. Different molecular weight averages such as Mn, Mw, Mp, Mz, Mz+1, Mv as well as polydispersity index can be found out using GPC as show in Figure 13.

Finally, the data was obtained from GPC within the form of a chromatogram showing detector response as a function of retention time for all different oligomers. All the fundamental parameters present in the chromatogram are shown in Figure 13.

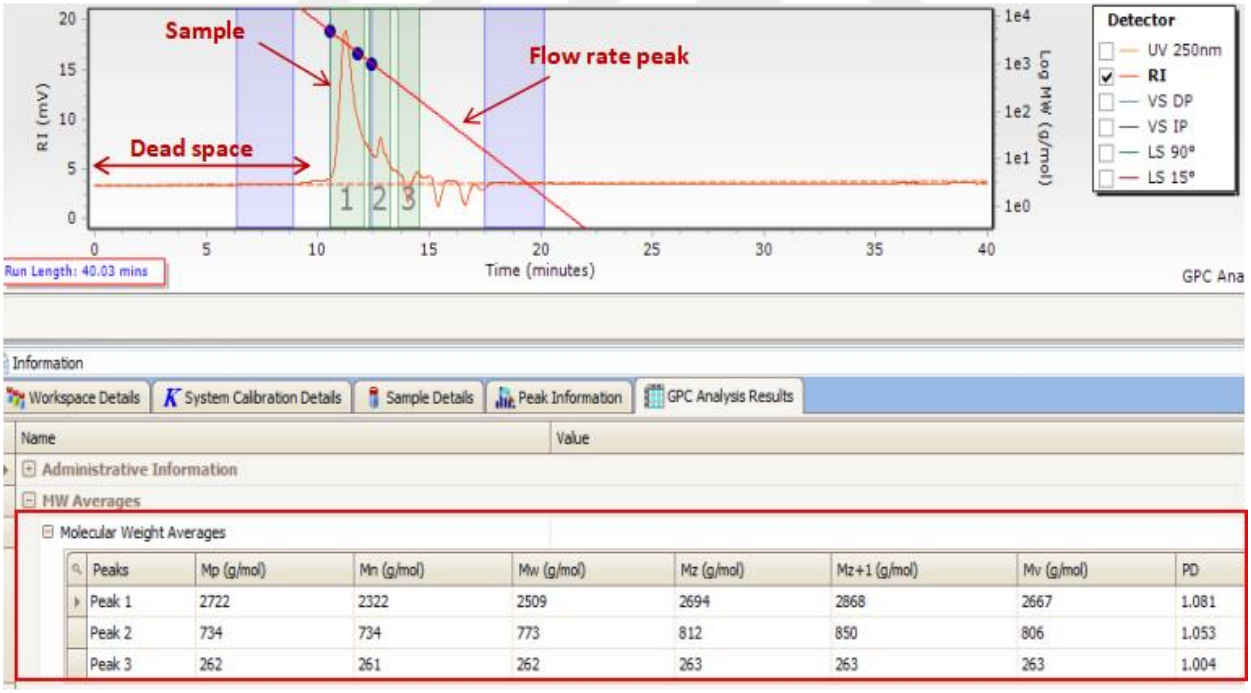

Peaks	Mp (g/mol)	Mn (g/mol)	Mw (g/mol)	Mz (g/mol)	Mz+1 (g/mol)	Mv (g/mol)	PD
Peak 1	2722	2322	2509	2694	2868	2667	1.081
Peak 2	734	734	773	812	850	806	1.053
Peak 3	262	261	262	263	263	263	1.004

Figure 13: A chromatogram obtained from Gel permeation chromatography (GPC) representing all components. Flow rate marker gives information about efficiency of chromatographic column. Dead space represents non-analytical region, peaks observed in this region indicate that sample has no interaction with stationary phase of column. The lower part of the figure highlighted in rectangular box shows types of average molecular weights that can be determined using GPC.

Chapter 3- Results and Discussion

3.1. Characterization of synthesized Oligomers-LCST and NMR Results

3.1.1. LCST Measurements

PNIPAM oligomers were synthesized by conventional free radical polymerization as well as by RAFT polymerization. PNIPAM synthesized via free radical polymerization was categorized into two different types: neutral and charged ones based on the initiator molecule utilized for synthesis. The synthetic route of these oligomers was described in the materials section (see section 2.2.1 & 2.2.2). The synthesized PNIPAM oligomers by both radical and RAFT polymerization was first characterized with the phase transition temperature (LCST) measurements (see Figure 14 below)

As seen from the graph, LCST of synthesized PNIPAM oligomer by radical polymerization with a charged end group has a value of 32.6 ℃ while the neutral end group has a value of 41.0 ^{0}C. The LCST for PNIPAM synthesized by RAFT polymerization is around 30.6^{0}C. Since this PNIPAM is not pure it also contains small amount of RAFT reagent that is sparingly soluble in water the sample below LCST was cloudy even at room temperature due to the bulky hydrophobic groups at the termini of the oligomer. Overall, all three synthetic routes gave rise to significant phase transitions at reasonable temperatures and thus it can be concluded that, from thermodynamic point of view the synthesis leads to polymerization.

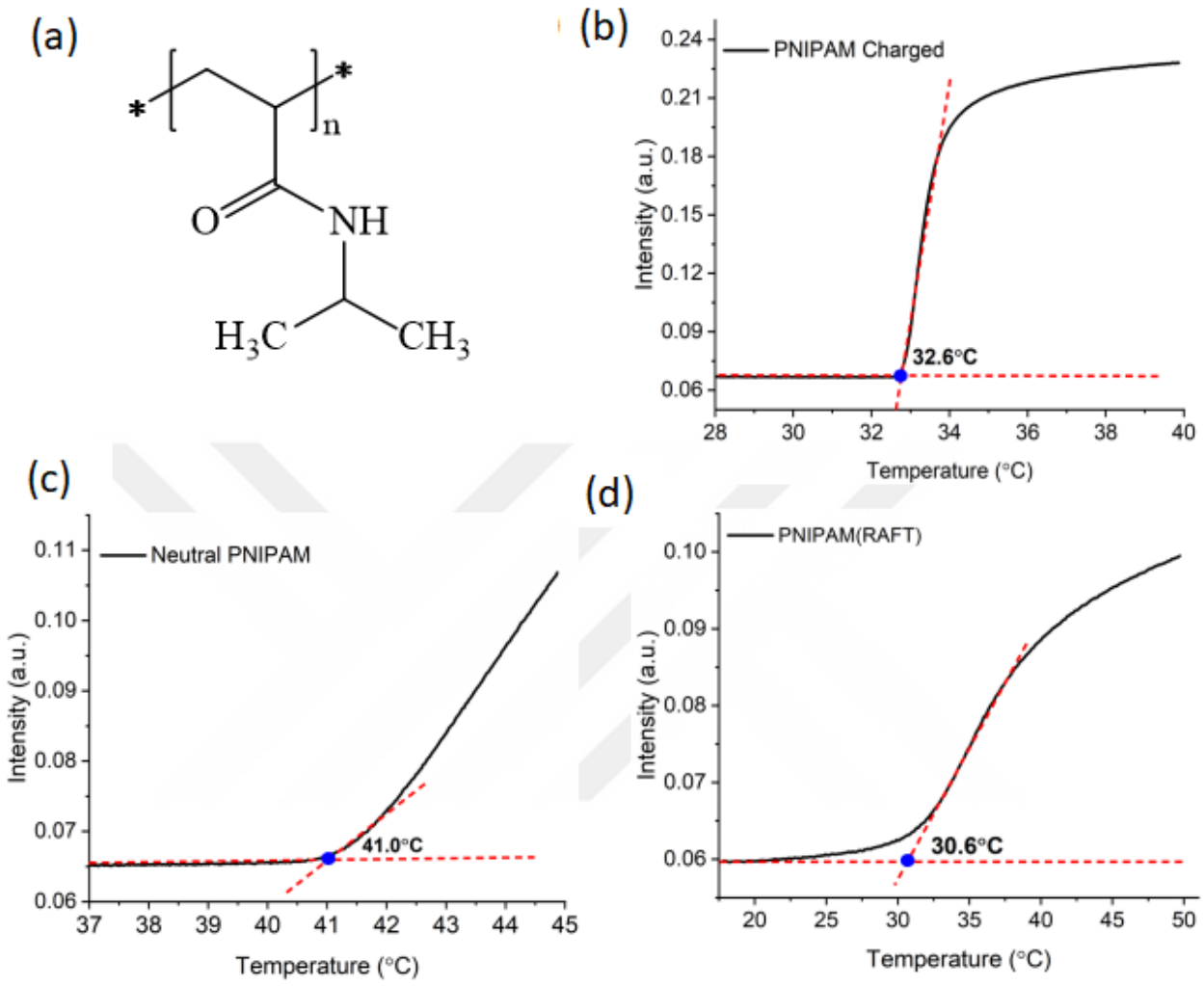

Figure 14: (a) Representative chemical structure of PNIPAM (b) LCST of PNIPAM with charged end-group (c) LCST of PNIPAM synthesized by radical polymerization with neutral end-group (d) LCST of LCST of charged end-group PNIPAM synthesized by RAFT polymerization. The LCST determination and the values are shown on the graph. The point which was taken for LCST is highlighted by a blue circle (●) on it. Approximately 10 mg/ml oligomer solutions in H_2O were measured for all measurements.

3.1.2. ^{1}H-NMR Results

The synthesized PNIPAM oligomers were also characterized by ^{1}H-NMR. The ^{1}H-NMR of monomer NIPAM and oligomers after synthesis was taken and compared to make sure no residual monomer to be left within the sample. (see Figures 15 and 16)

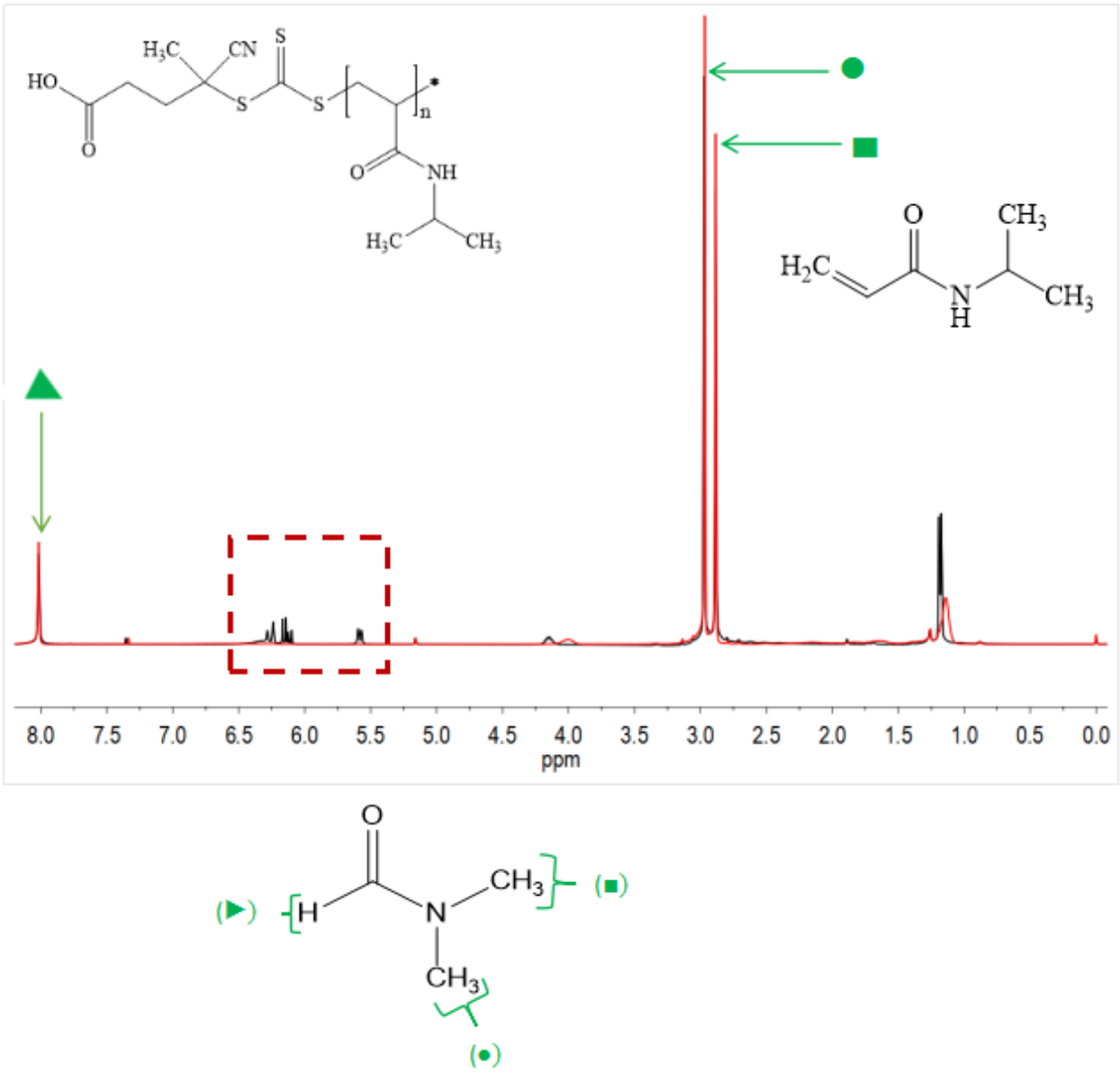

Figure 15: : [1]H-NMR of PNIPAM Oligomers synthesized by RAFT polymerization. The graph shown in black is for monomers while in red is of Oligomers. The region 5.4-6.5ppm highlighted in the rectangular box is for double bond protons of the monomers. The absence of these peaks in the oligomer's spectrum emphasizes successful polymerization. The peaks labeled with green geometric shapes belong to 3 sets of protons of DMF solvent, whose structure is also given. The remaining chemical shifts corresponds to the oligomers.

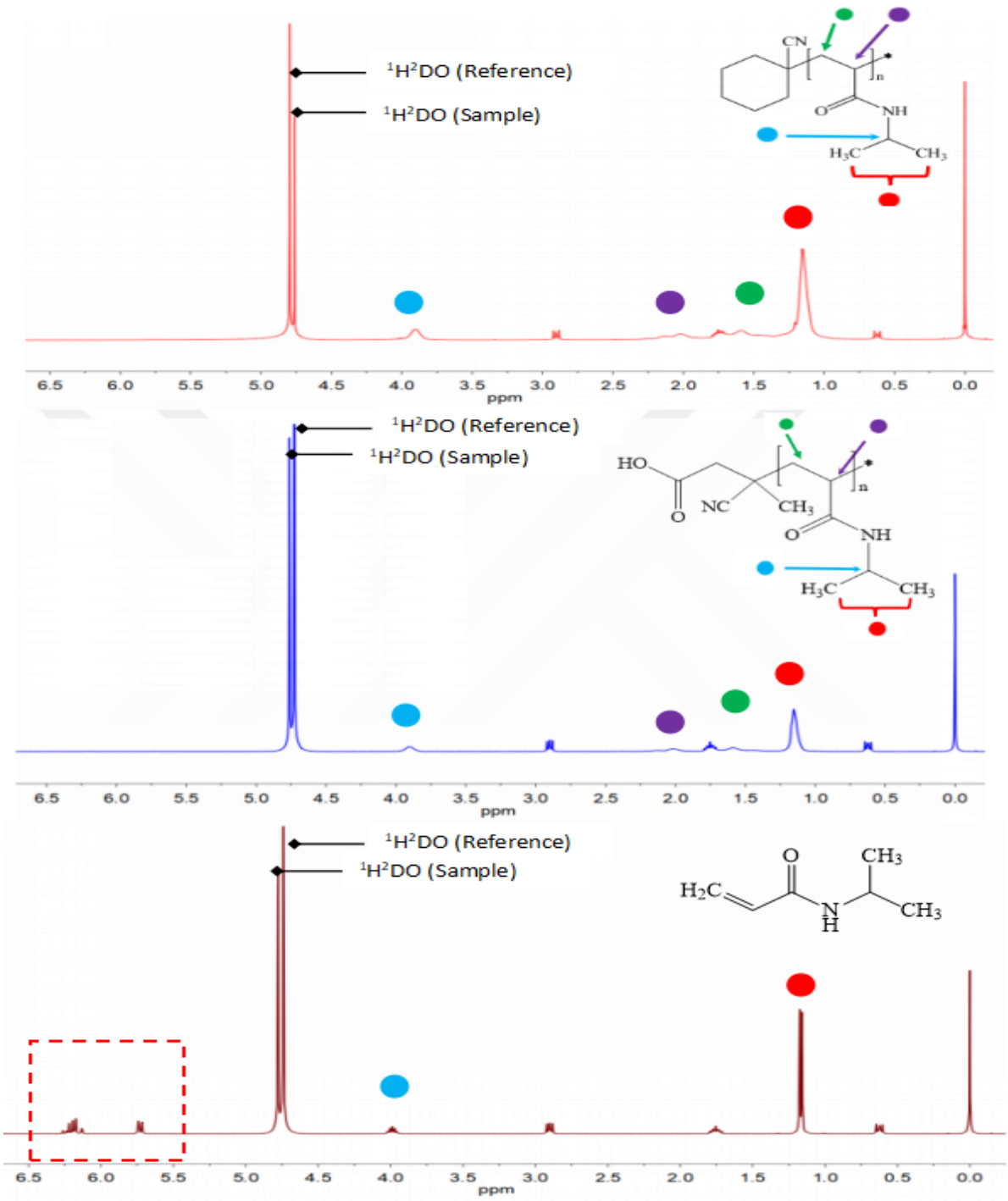

Figure 16: The representative ^{1}H-NMR spectra of PNIPAM monomer and Oligomers (charged and neutral end group) arranged from bottom (monomer), middle (charged end group) and top (neutral end group) synthesized by radical polymerization. Chemical structure relative to each spectrum is given on spectra. The color-coded protons in the structure (in the middle and top) are labeled with the same color on each spectra to represent that type of proton in each structure.

The ^{1}H-NMR spectra of PNIPAM oligomers synthesized by RAFT polymerization was taken in DMF so peaks at 3.1-3.4ppm and at 8.0 ppm corresponds to solvent. While the NMR of free radical synthesized is taken in D_2O by method of external reference, the peaks in region 4.7-5.00 ppm correspond to D_2O while peak at 0 (zero) refers to reference DSS as shown in Figure 16. The color-coded protons in the structure (in the middle and top) are labeled with the same color on each spectra to represent that type of proton in each structure.

Figure 16 shows two ^{1}H-NMR spectra, the NIPAM monomer and PNIPAM Oligomers. The highlighted region in red box is between 5.5 and 6.5 ppm which show chemical shifts for hydrogens adjacent to double bond of the monomer. These peaks are clearly visible in the spectra of monomer sample, as NIPAM has three hydrogens adjacent to two carbons joined with a double bond. (as labeled with different colors in the chemical structure of NIPAM and on the NMR spectra) These peaks are however absent in the oligomer's spectra. This disappearance of peaks in the spectra of oligomers provide another evidence for successful polymerization reaction.

3.1.3. Molecular Weight Determination

The gel permeation chromatography (GPC) experiments were utilized to determine the relative molecular weight of synthesized PNIPAM oligomers. The samples were carried out with stabilized THF as mobile phase. Polystyrene (PS) and polymethylmethacrylate (PMMA) narrow polydispersity standards were both employed to reach a calibration curve of the elution time. A common experiment was performed as follows. First, only THF solvent run through the column as eluent to check the performance of the column. Then the samples were loaded and its elution time was measured. Then, the reference such as polystyrene (PS) and polymethylmethacrylate (PMMA) were loaded and elution time was measured. After this calibration curve as shown in the figure 17 (A red line with points on graph) was formed and compare with sample and molecular weight was determined via refractive index vs retention time chromatograms that are shown in the Figures 17, 18, and 19 obtained for three different oligomers.

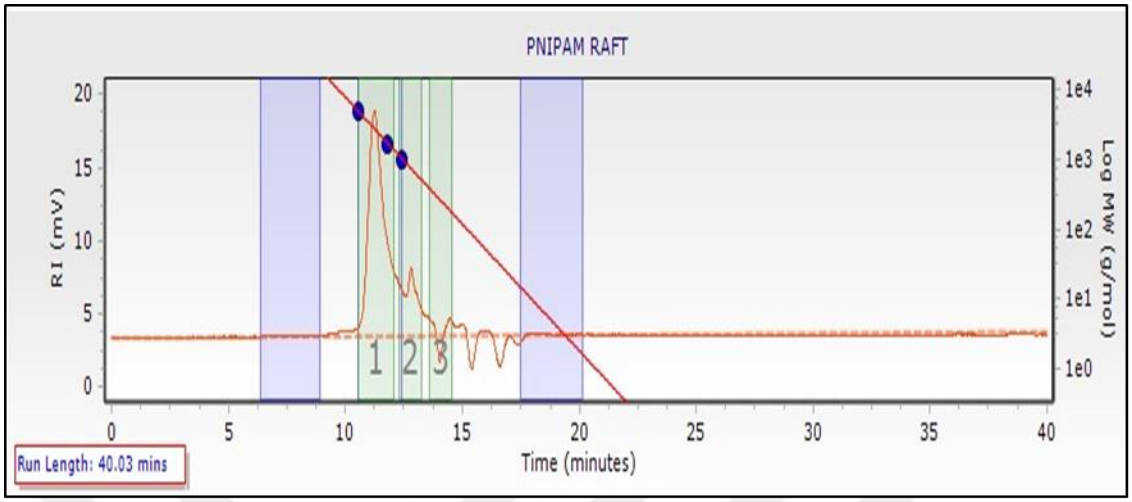

Peaks	Mp (g/mol)	Mn (g/mol)	Mw (g/mol)	Mz (g/mol)	Mz+1 (g/mol)	Mv (g/mol)	PD
Peak 1	2722	2322	2509	2694	2868	2667	1.081
Peak 2	734	734	773	812	850	806	1.053
Peak 3	262	261	262	263	263	263	1.004

Figure 17:A Chromatogram **(**Plot of refractive index vs retention time) for PNIPAM oligomer polymerize by RAFT polymerization method. Blue vertical line on the graph is calibration curve constructed by using well defined Polymethylmethacrylate (PMMA) references of molecular weights (Mp=1010 g/mol, 1710 g/mol, 4920 g/mol). The dots represent the references. The number in grey 1,2 & 3 show the number of peaks. The peak one from sample has Mp = 2722 g/mol, peak 2 has Mp= 734 g/mol and peak 3 has Mp=262 g/mol.

The molecular weight of PNIPAM oligomers synthesized by RAFT polymerization has a molecular weight of 2509 g/mol, while the calibration curve was generated using Polymethylmethacrylate standards. The obtained molecular weight with PMMA as standard was 2509 g/mol as shown in Figure 17, that is inline with polystyrene based measurements. The molecular weight was also determined via using polystyrene (PS) standards with known molecular weights (Mp:575 g/mol, 1530 g/mol, 3950 g/mol, 29510 g/mol, 205,000 g/mol, 72450 g/mol, 10210 g/mol). The molecular weight using PMMA was 2611 g/mol Since, there is an estimated the molecular weight value of the oligomer sample smaller number of PMMA standards were employed. As can be seen either standards can be utilized to determine the molecular weight of the oligomer samples.

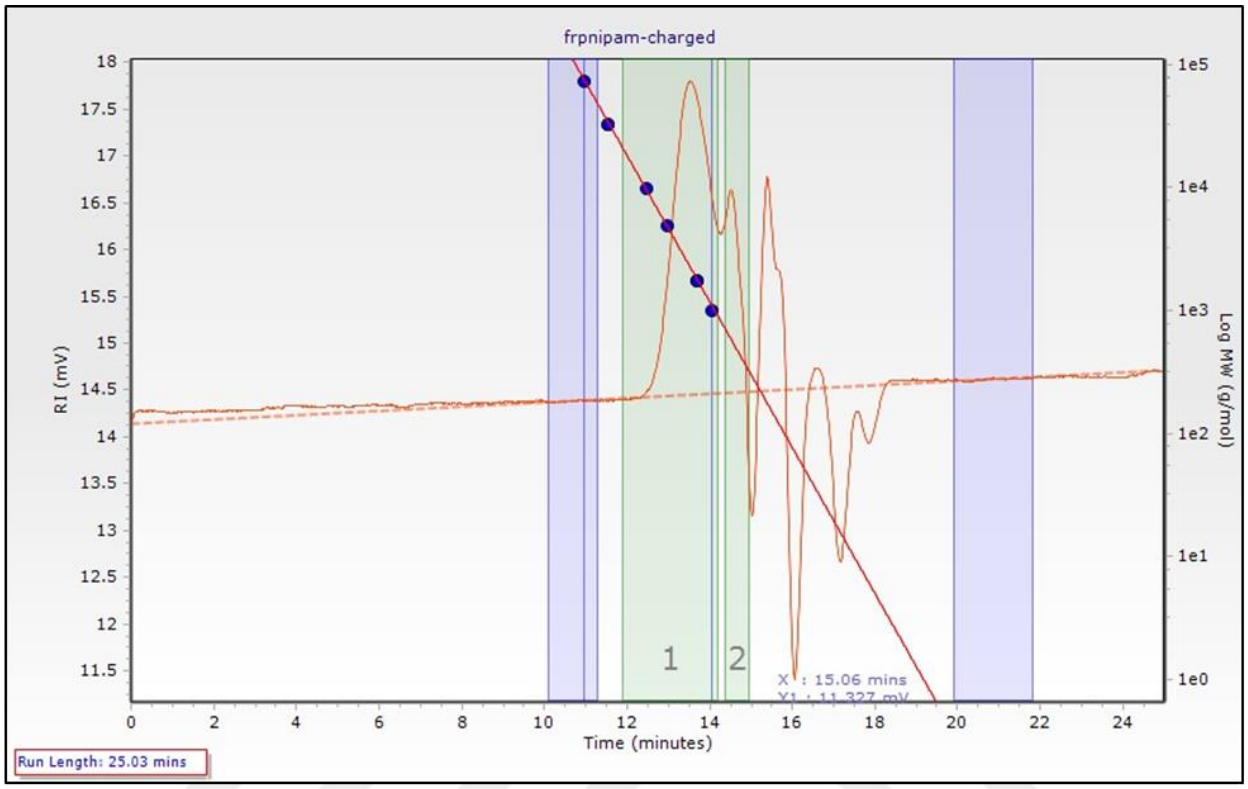

Peaks	Mp (g/mol)	Mn (g/mol)	Mw (g/mol)	Mz (g/mol)	Mz+1 (g/mol)	Mv (g/mol)
Peak 1	2192	1912	2458	3191	4053	3072
Peak 2	572	521	536	550	564	548

Figure 18: A chromatogram (refractive index vs retention time) for PNIPAM synthesized by radical polymerization with a charged end group. Red line with blue points demonstrates the calibration curve obtained by using the standard of PMMA with defined molecular weights (Mp = 1010, 1760, 72800, 32340, 4920 and 9720 g/mol). For the sample the Mp obtained was Mp =2192g/mol for peak 1 and Mp= 572g/mol for peak 2.

The molecular weight of PNIPAM oligomers with charged end groups synthesized by radical polymerization was measured using polymethymethacrylate (PMMA) as standards is shown in Figure 18. The obtained molecular weight using PMMA standards was 2458 g/mol. However, when it was measured using polystyrene (PS) as reference (Mp = 580, 2946, 1180, 9310, 4680, 75050 g/mol) the obtained molecular weight was 1955 g/mol. Again quite similar results were achieved when different standards were employed.

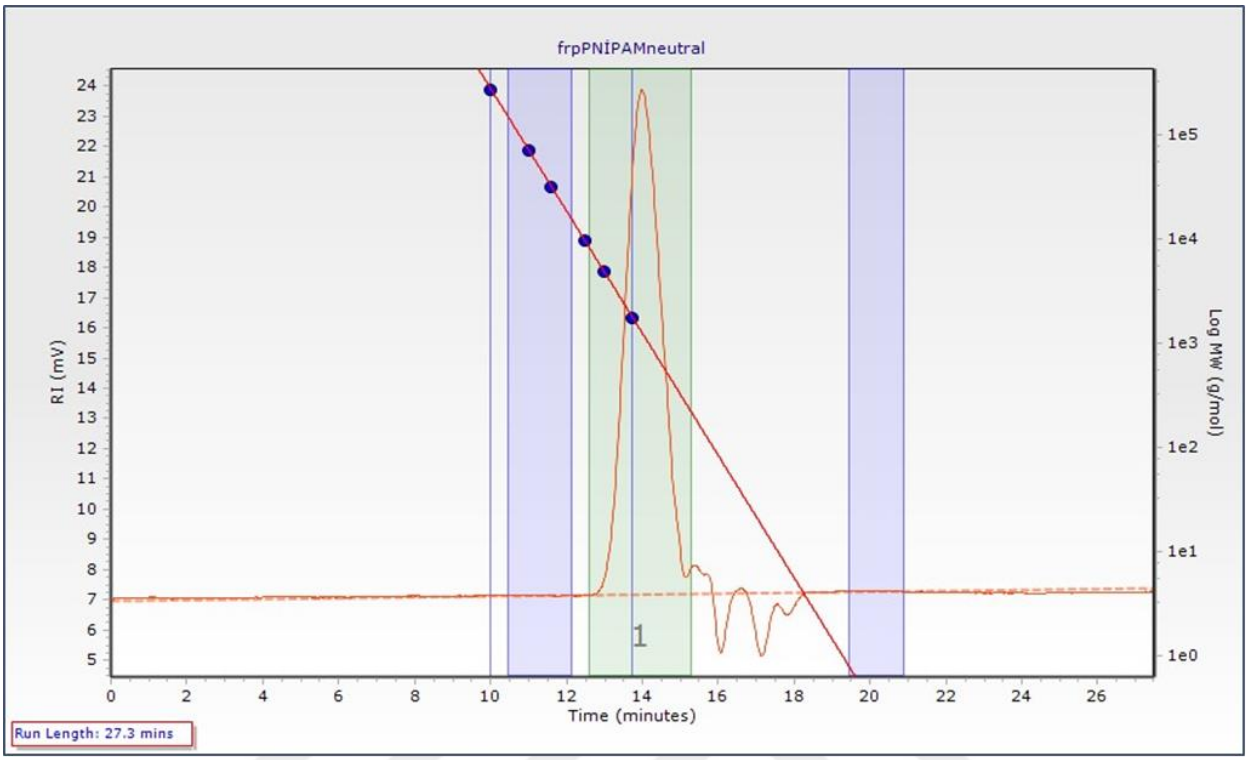

Peaks	Mp (g/mol)	Mn (g/mol)	Mw (g/mol)	Mz (g/mol)	Mz+1 (g/mol)	Mv (g/mol)
Peak 1	1260	985	1372	1838	2345	1766

Figure 19: Chromatogram obtained from GPC by using refractive index detector where refractive index is plotted as function of retention time for PNIPAM with neutral end group polymerized by radical polymerization. The calibration curve (marked on graph in red color with blue points) was constructed by using standard PMMA with known molecular weights (Mp = 1760, 4920, 9720, 32340, 72800,27360 g/mol). The Mp result for the sample is Mp = 1260 g/mol.

The molecular weight of PNIPAM oligomer with neutral end group was measure only using PMMA standard. The PMMA standards use to create calibration curve were Mp = 1760, 4920, 9720, 32340, 72800 and 27360 g/mol. The calibration curve demonstrated on graph in Figure 19 is constructed of these standards. The obtained molecular weight of neutral end group oligomer was Mw =1372 g/mol.

The molecular weight of all synthesized oligomers of PNIPAM by RAFT and radical polymerization with other properties like LCST, type of initiator used in polymerization (two

different initiators ACVA & ABCN), method of polymerization and solvent used are tabulated in Table 1.

Table 1: Summary of synthesized Oligomers: Synthesis methods, Initiator, LCST and calculated molecular weights.

Polymer	**Method of synthesis**	**Initiator used**	**Mol.wt (M_w) g/mol**	**LCST**	**Solvent**
PNIPAM	RAFT.poly	Charged (ACVA)	2611- STY 2509-PMMA	30.6	DMF
PNIPAM	Radical.poly	Charged (ACVA)	2285-PMMA 2458-PMMA 1955-STY	32.6	Methanol
PNIPAM	Radical.poly	Neutral (ABCN)	1372-PMMA	41.0	IPA
PNIPAM	Radical.poly	Neutral (ABCN)	1556-PMMA 1491-PMMA 1221-STY	37.4	IPA
PNIPAM	Radical.poly	Neutral (ABCN)	1346-STY 1665-PMMA	37.32	IPA
PNIPAM	Radical.poly	Neutral (ABCN)	2151-PMMA	34	IPA

IPA=Isopropyl alcohol, DMF=Dimethylformamide, PMMA=Polymethylmethacrylate, STY=Polystyrene, Charged initiator= 4,4'-Azobis(4-cyanovaleric acid) (ACVA), Neutral initiator=1,1'-Azobis(cyclohexanecarbonitrile) (ABCN).

3.2.Titration with Weakly and Strongly hydrated anion

After the synthesis of PNIPAM oligomers with charged and neutral end groups, we study the influence of specific ion effects on the solution phase properties of these oligomers. The effect of Hofmeister ions on neutral polymers as a function of molecular weight has been studied by Cremer and coworkers by using polyethylene glycol (PEG) as a model compound.[41] They employed oligomers and polymers of varying molecular weight to determine how the molecular size effect influences the ion – macromolecule interactions. In order to demonstrate the relation between interfacial water structure and Hofmeister ion binding, the concepts of hydration, molecular surface curvature have been utilized. Significantly distinct trends were observed for surface adsorption of weakly hydrated anion, i.e. SCN^- and the structure of water molecules in the hydration shell along the chain length. Water molecules near the termini display a higher degree of tetrahedral ordering. In contrast, at the center of the chain they exhibit weaker and less

tetrahedral arranged hydrogen bonds. The strong affinity for SCN^- ions for binding has been observed at the sites where disordered hydrogen bonding is dominating. Stillinger and coworkers visualized that hydrogen bonding of water molecules is similar to bulk phase around small molecules whereas in large solutes it undergoes disruption near the surface, more closely mimicking the air/water interface.[121] The chain length and site specificity of anions adsorption and hydration structure is not only studied for NaSCN and PEOs.

In this part, the ion specificity for amide-based oligomer containing neutral end groups will be discussed. Weakly hydrated anions generally show no binding affinity to monomers but prefer to bind to polymer and oligomers. The amide-based oligomers synthesized in this thesis are expected to demonstrate similar trends to PEG. As we can see in the Figure 20 the LCST of PNIPAM in the presence of weakly hydrated anion such as SCN^- show a nonlinear trend as a function of anion concentration. A non-linear curve reflecting a Langmuir binding isotherm behavior is coupled with a decreasing trend. This implies that two opposing effect a salting in via ion – binding and salting out with presence of ions. Using equation 04 one can measure the empirical dissociation constant (K_D), with a $K_D = 1.14 \pm 0.07$ M. In the case of sodium salts of strongly hydrated anions such as Cl^-, there is no apparent binding, a monotonic salting out effect can be seen evident by the linear decrease in LCST as a function of salt concentration.

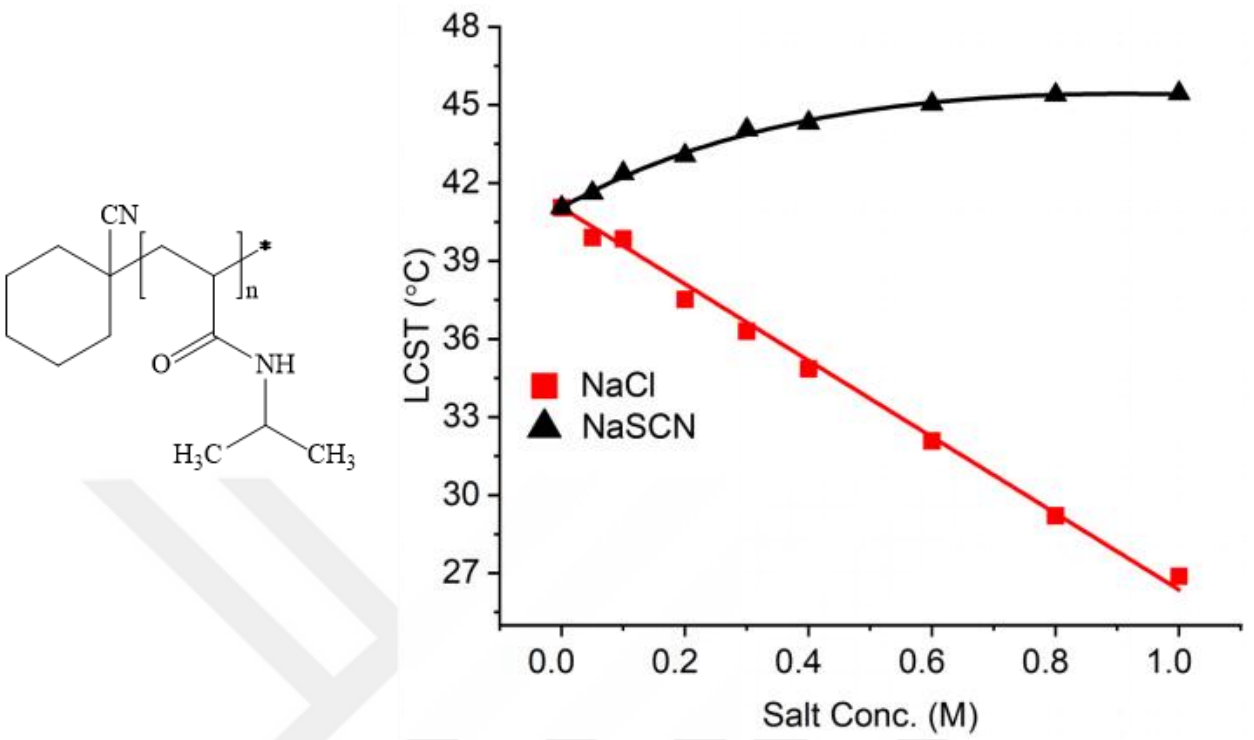

Figure 20: (Left). The Chemical structure of neutral end group PNIPAM Oligomers. (Right). Fitted Lower Critical Solution Temperature (LCST) of PNIPAM (Neutral) Oligomers as a function of varying concentration of two salts. LCST are measured in aqueous solution by using salt as cosolutes.

Similar analysis has been performed for PNIPAM oligomers with charged end-group. The effect of specific ion effects on charged end group oligomers by the LCST measurement. LCST has been measured as a function of the same sodium salts of strongly and weakly hydrated anions. As we can see in Figure 21 the strongly hydrated anion has no tendency to bind and directly salt-out the polymer, whereas the weakly hydrated anion, SCN^-, show ion binding behavior with an apparent $K_D = 0.58 \pm 0.1$ M. The ion binding to small molecules to oligomers that include charge is relatively sparsely studied concept. The effect of salts on charged small molecules has been demonstrated by Paterova *et al*. for capped and uncapped trigylcine and explained that traditional explanation of mechanism of ordering of Hofmeister ions in terms of bulk hydration is not sufficient to explain the solution properties of triglycine. With the help of ^{1}H-NMR spectroscopy and MD simulation it is shown that uncapping of N-terminus makes the Hofmeister ordering to reverse. Whereas, the strongly hydrated anions show no binding while weakly hydrated anions such as I^- and SCN^- had some weak binding with $K_D > 1$ M. Please note that, such studies have not been performed for any

oligomers holding charge groups. As such, there is still no clear explanation for ion interactions with oligomers with charged end group.

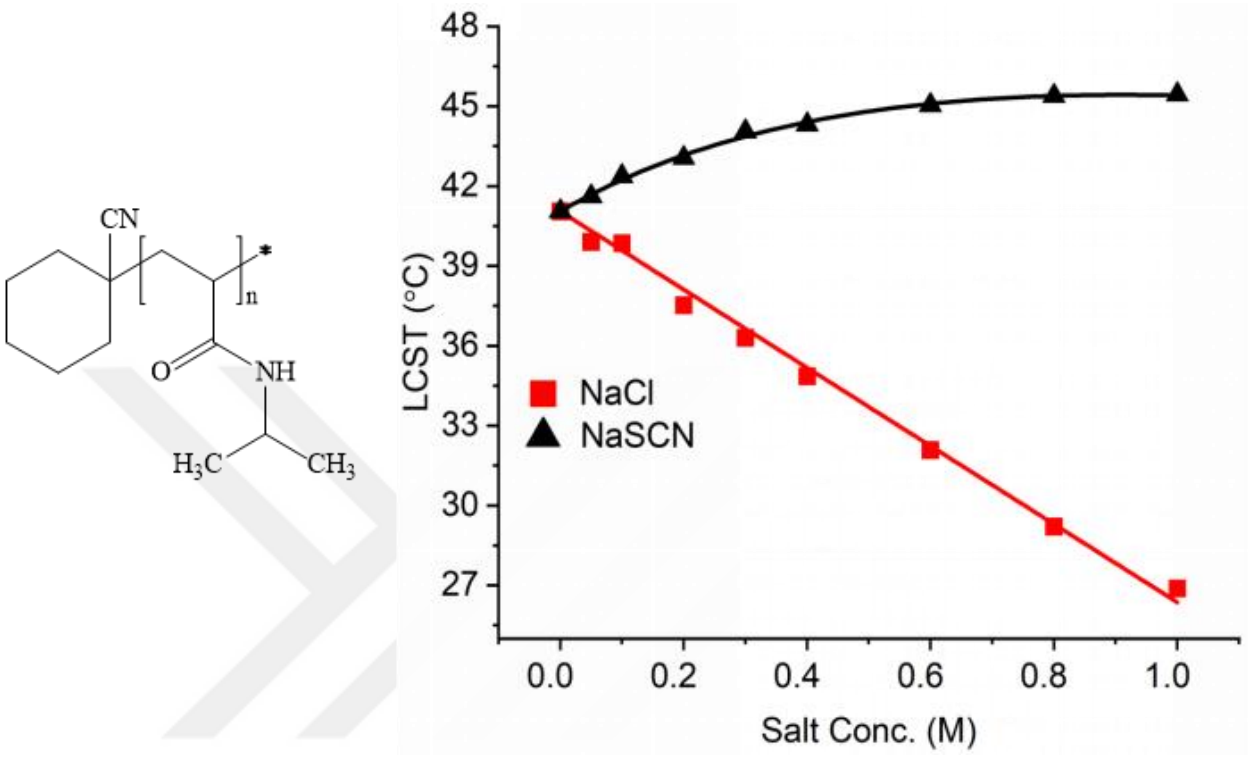

Figure 21: (Left). The Chemical structure of charged end group PNIPAM Oligomers. (Right). Fitted Lower Critical Solution Temperature (LCST) of PNIPAM (Charged) Oligomers as a function of varying concentration of two salt as cosolutes in aqueous solution.

Ion influences on the phase transition of PNIPAM oligomers (both neutral and charged) has been modeled to an empirical equation that contains a linear term and Langmuir binding isotherm, see below[118]

$$T = T_0 + c\,[M] + \frac{B_{max}\,[M]}{K_D + [M]} \qquad (4)$$

T_0, is the phase transition temperature in the absence of salt, and c, the slope of the linear term, has units of temperature/concentration (°C/[M]), that describes the linear salting-out efficacy of a specific salt. The nonlinear term describes the Langmuir-type binding interaction with a coefficient B_{max}, which corresponds to the maximum increase in the phase transition temperature. K_D is the apparent equilibrium ion dissociation constant. Equation 4 can be used to model the phase transition data for all employed salts. For strongly-hydrated anions, the apparent binding

interaction is relatively weak (K_D >> 1 M) and thus no nonlinear contribution is present. For the salts of weakly hydrated anions, the apparent non linearity can be fit by the Langmuir binding isotherm. The evident K_D values range from 0.5 M – 1 M, and follows the order below. Table 2 shows the fitting parameters for all salts. The phase transition temperature measurements clearly indicate a direct ion-oligomer interaction is occurring for PNIPAM. Yet, the phase transition temperature measurements only report on the solution phase properties of the macromolecule, and cannot report on the actual binding site of the anions. In order to achieve molecular-level details on the influence of ions on the sugar-based macromolecules, systematic ^{1}H-NMR measurements are needed.

Table 2: Fit values of the parameter for c, K_D, B_{max} from equation 04 for both neutral end group and charged end group PNIPAM oligomers for two salt NaSCN and NaCl.

Salt	Concentration range	C ($K.M^{-1}$)	K_D (M)	B_{max} (K)
PNIPAM-Neutral end group				
NaCl	0-1.0 M	14.68	-	-
NaSCN	0-1.0 M	6.0	1.13	22.15
PNIPAM-Charged end group				
NaCl	0-1.0 M	12.74	-	-
NaSCN	0-1.0 M	6.05	0.57	9.38

3.3. SUMMARY-Synthesis of PNIPAM Oligomers and their interaction with Hofmeister Ions.

In the first part of this thesis PNIPAM oligomers were synthesized by RAFT and radical polymerization. The oligomers synthesized by radical polymerization were of two types depending on type of initiator used for synthesis; one with the charged end group and other with neutral end group. Then, the effect of introduction of 2 salts (NaCl & NaSCN) on the phase transition temperature of these PNIPAM oligomers, synthesized by radical polymerization was studied. In the case of charged oligomers equilibrium dissociation constant is $K_D = 0.58 \pm 0.07$ M indicating the weak binding of weakly hydrated anions to oligomers. In case of charged oligomer, the equilibrium dissociation constant of $K_D = 1.14 \pm 0.07$ M was calculated, which shows that neutral oligomers have even much weaker binding compared to charged one. As can be seen in the figure, weakly hydrated anions show no binding to small molecules such as monomers (literature[41]) and

have weak binding with oligomers (this thesis and literature[41]). These anions show stronger binding with large macromolecules as shown by polyethylene glycol[41] PNIPAM[122], elastin like polypeptides[100,101] of different molecular weights.

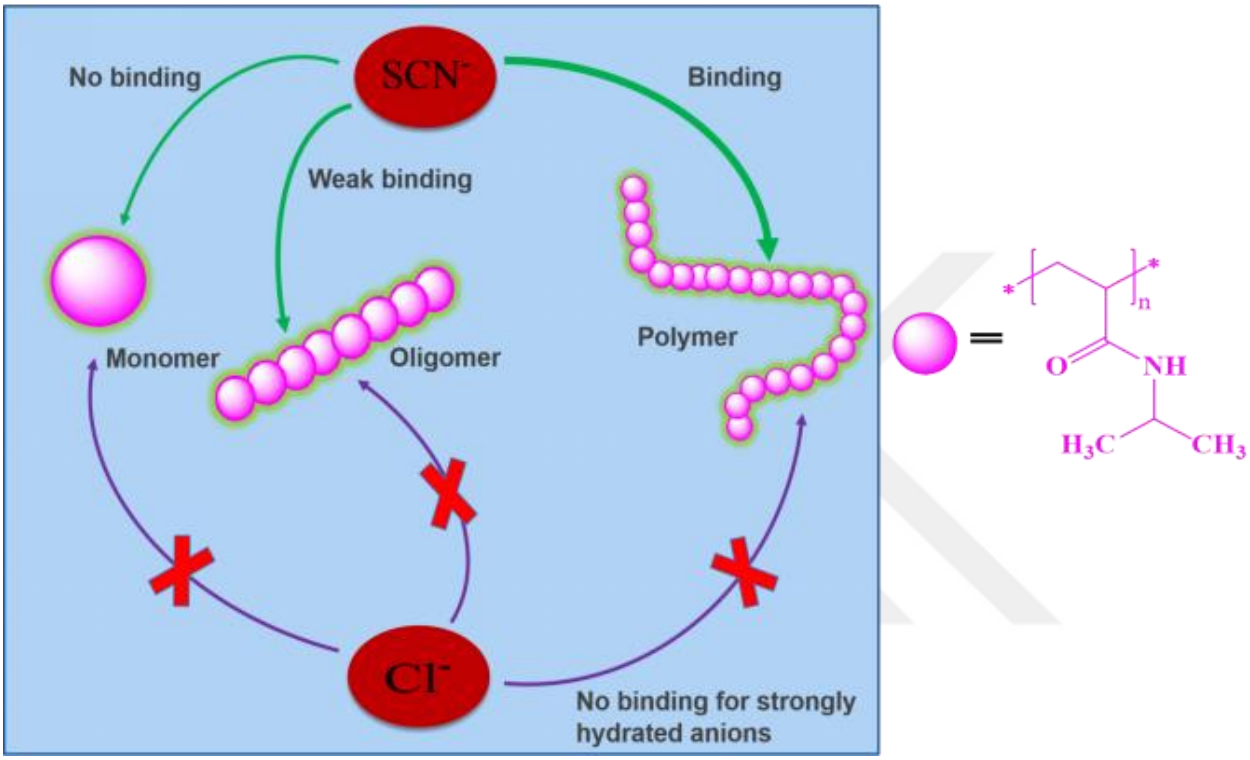

Figure 22: Graphical representation of the main summary for first part of this work: the molecular mechanism for the binding and nonbinding behaviour of weakly hydrated (SCN^-)and strong hydrated (Cl^-) ions on neutral end group PNIPAM oligomer, monomer and polymer. The mechanism for the monomer and polymer of PNIPAM is adopted from literature.[41,122,100,101]

3.4. Hofmeister Ions and Sugar Macromolecules

As we have discussed in the previous section, the Hofmeister effect has been well explained for polymers but many other physiological macromolecules such as sugar-based macromolecules which are an important component of cell membrane also demonstrated the Hofmeister effect. In this section we will discuss the effect of these ions on sugar-based macromolecules, specifically Hydroxypropylcellulose (HPC). HPC is a derivative of cellulose. Since cellulose is insoluble in water while this derivative of cellulose is water soluble. HPC is thermoresponsive like amide-

based polymer and have wide range of application in drug delivery because of bio-compatibility.in the upcoming section we will discuss the effect of addition of Hofmeister ion on HPC by using LCST measurement and to demonstrate site specific binding we will use NMR spectroscopy.

3.4.1. LCST Measurements: Evidence of Hofmeister Effect

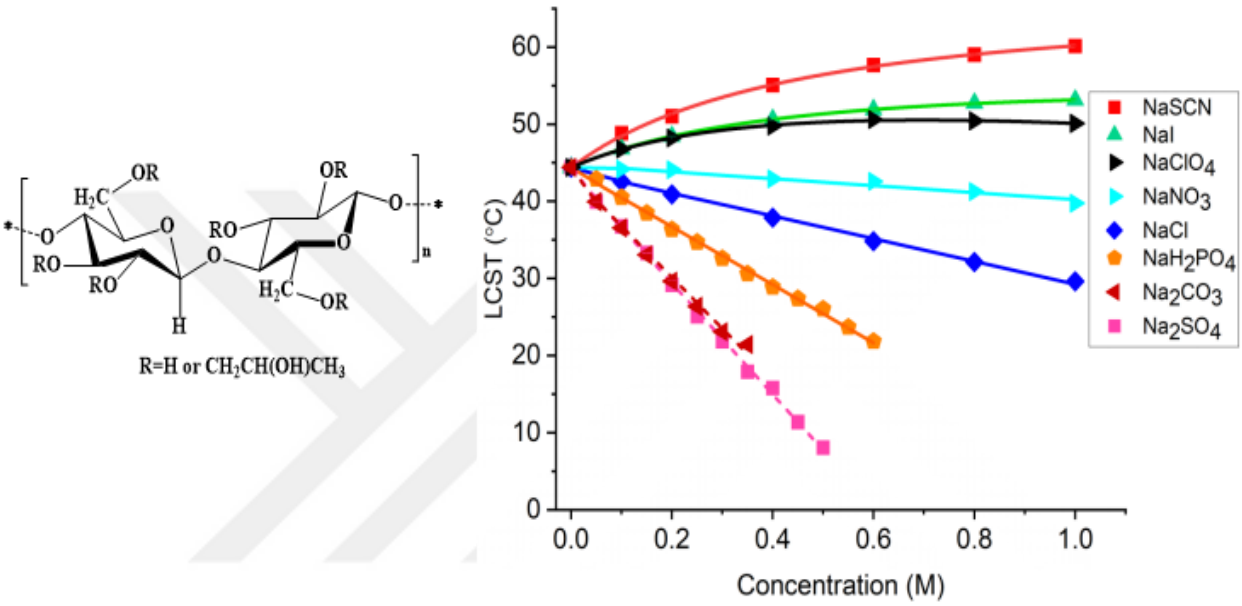

Figure 23: (Left). The chemical structure of Hydroxypropyl cellulose (HPC). (Right). Fitted phase transition temperatures curves for HPC as a function of varying concentration of 8 different sodium salts used as cosolutes in aqueous solution. The dotted line in case of Na_2SO_4 and Na_2CO_3 shows LCST split into two step transition for both salts.

Figure 23 shows the initial onset values of the phase transition temperature for HPC solutions as a function of salt concentration of both monovalent and divalent anions studied for 8 sodium salts. In the absence of salts, the phase transition for HPC occurred at 44.3 ± 0.4 °C. The presence of salt ions specifically influences the phase transition temperature. In the presence of four strongly hydrated anions (CO_3^{2-}, SO_4^{2-}, $H_2PO_4^-$, Cl^-) the phase transition temperature linearly decreases with increased salt concentrations. These salts are ranked in the following order according to their ability to decrease the phase transition temperature:$CO_3^{2-} > SO_4^{2-} > H_2PO_4^- > Cl^-$. The LCST for high concentration of these anions proceeds in two different steps demonstrated in Figure 24 (b) in contrast to single step transition shown in Figure 24 (a), as it has been observed in case of

PNIPAM.[123] In contrast, the sodium salts of weakly hydrated anions have quite different effects. For these anions (NO_3^-, ClO_4^-, I^-, SCN^-), the effect on phase transition temperature is nonlinear.

The high concentration of strongly hydrated anions such as CO_3^{2-} and SO_4^{2-} influenced the phase transition temperature of HPC in quite intricate manner. There is a linear correlation between solubility of HPC and concentration of anions. But as the concentration of anions increases, a sudden change in slope is observed. This behaviour causes the phase transition to be resolved into low and high temperature transitions as shown by two phase transitions for Na_2SO_4 solution in figure. At Na_2SO_4 below 0.15M single phase transition is evident, but higher concentrations lead to two distinct phase transitions. The plots of temperature for high and low temperature phase transition for strongly hydrated anions such as Na_2SO_4 and Na_2CO_3 are demonstrated in Figure 25 shows that individual steps have different slopes. The phase transitions at lower temperature have more pronounced dependence on salt concentration and have steeper slope while higher temperature phase transitions have profoundly shallower slope. Ion influences on the phase transition of neutral macromolecules were modeled to an empirical equation 4 that contains a linear term and Langmuir binding isotherm as explained in the previous section.

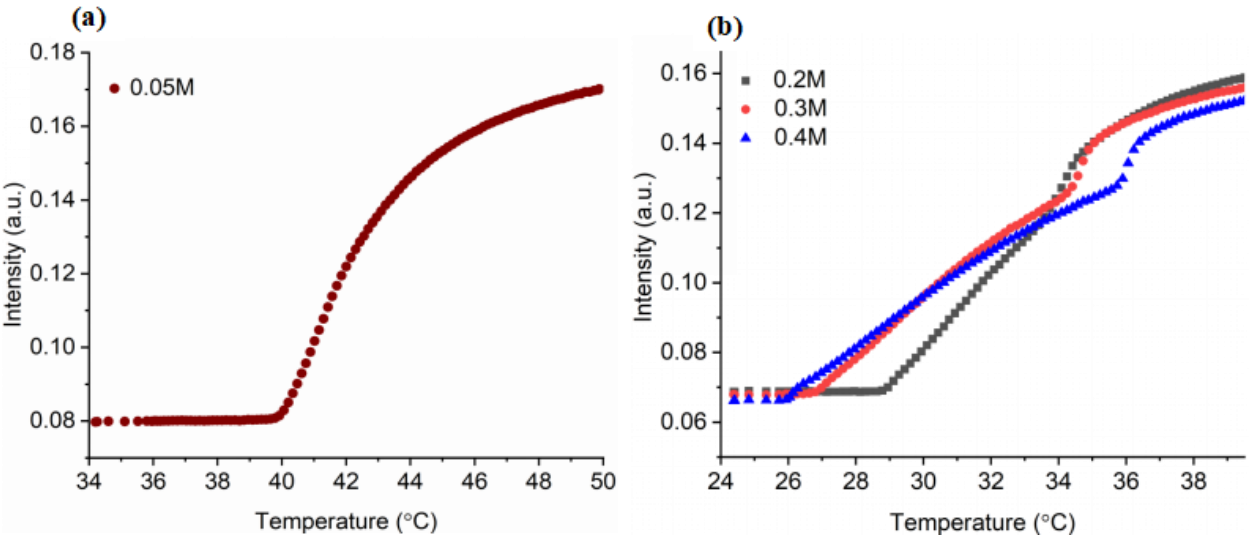

Figure 24: Phase transition temperature (LCST) of HPC in aqueous solution with varying concentrations of Na_2SO_4 as cosolutes: (a) One step phase transition. (b) The two-step phase transition is particularly observable at 0.2 M and above.

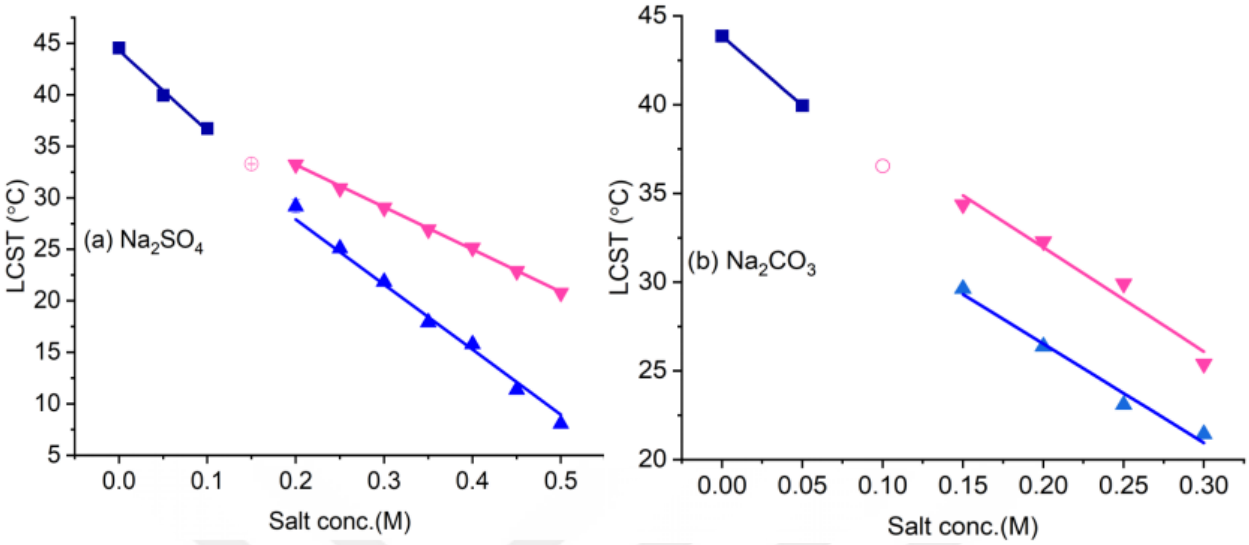

Figure 25: Plot of phase transition temperature vs salt concentration for strongly hydrated anions. (a). Na_2SO_4 (b). Na_2CO_3. initial slope (Royal blue, ■). Lower temperature step in two step phase transition (blue, ►). Higher temperature phase transition (pink, ◄). (○, pink) denotes the junction at which phase transition broadens without distinctly separating into two separate steps. It marks the shift of phase transition from single to double steps.

The constant c in the equation 4 which has the unit of temperature/molarity is directly related to hydration entropy of anions in case of phase transition for strongly hydrated anions. On the other hand for weakly hydrated anions and for second transition in case of strongly hydrated anions, change in surface tension σ of anions with increasing salt concentration is the dominant mechanism and c is proportional to the surface tension. The weak binding of weakly hydrated anions also affects the solubility of HPC for that third term in the equation is needed where K_D is the apparent binding constant for anions to the HPC. B_{max} indicates the increase in phase transition temperature due to binding at saturation. The solid lines in the Figure 23 fit to the data according to this modeled equation 4. The abstracted K_D, B_{max}, and c values are shown in the table 3 for all anions.

In a two-step phase transition for strongly hydrated anions, the first step transition can be correlated to the hydrated entropy of anions, which suggests the dehydration of hydroxyl group by polarization effect. In this case more strongly hydrated anion will polarize the water molecules surrounding the HPC which leads to dehydration. The lower temperature phase transition is due to the disturbance of water molecules in the solvation of HPC rather than interaction with

hydrophobic portion of sugar macromolecule and was tested by solvent isotope studies. It is observed that isotope effect is different for each step of two step phase transition. For instance, it can be seen by the difference in transition of HPC with 0.3M Na_2SO_4. Both transitions show an increase in temperature in D_2O. But the magnitude of shift for the lower temperature transition (~0.99^0C) is double that of the shift at higher temperature (~0.49^0C) illustrated in Figure 26(a). This significant difference indicates the involvement of H-bonds being broken in first step transition at lower temperature. As deuterium bond is D_2O is around 5% stronger than H-bond in H_2O which leads to an increase in phase transition temperature on enthalpic grounds. The elucidation of results presented herein in case of 2 step phase transition is grounded in the literature[123] that pertains to PNIPAM. The rationale for this linkage arises from the analogous observations documented in PNIPAM studies, where a similar phenomenon was noted as shown in Figure 26 (b).

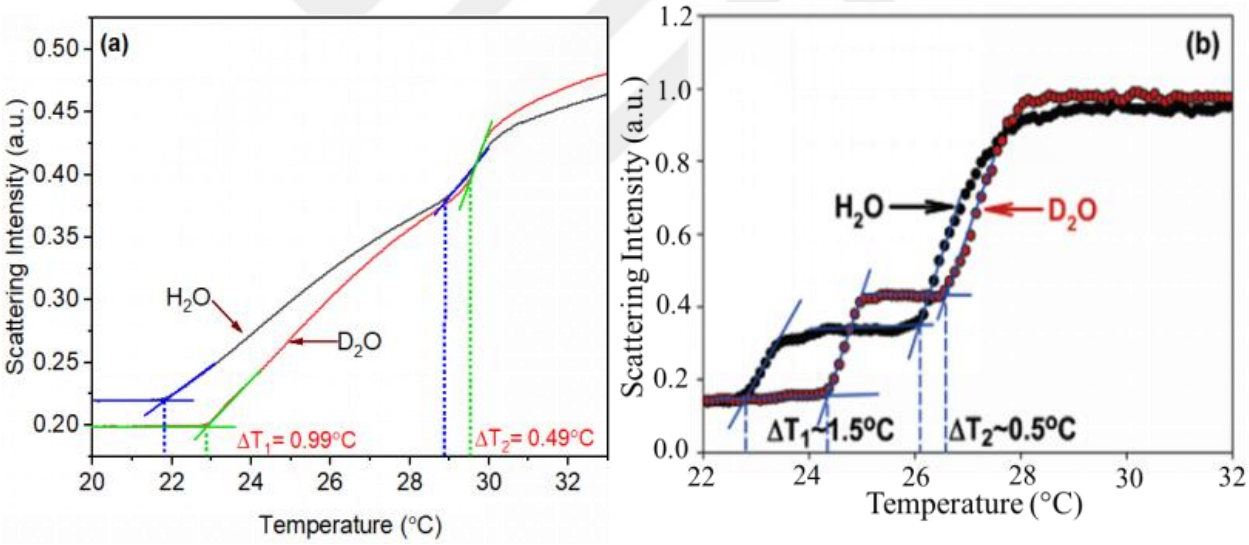

Figure 26: (a)Temperature vs scattering Intensity curve for HPC and Na_2SO_4 in H_2O and D_2O. (b) Comparison of two transitions in H_{2O} and D_2O for PNIAPM[123] and Na_2SO_4.

Yet, the phase transition temperature measurements only report on the solution phase properties of the macromolecule, and cannot report on the actual binding site of the anions. In order to achieve molecular-level details on the influence of ions on the sugar-based macromolecules, systematic ^{1}H-NMR measurements were performed. ^{1}H-NMR can provide chemical-specific information.

Table 3: Fit values of parameter for c, K_D, B_{max} from equation 04 for HPC with 8 different salts.

Salt	Concentration range	C ($K.M^{-1}$)	K_D (M)	B_{max} (K)
NaSCN	0-1.0 M	0.6 ± 3.1	0.4 ± 0.1	24.4 ± 6.8
NaI	0-1.0 M	2.17± 0.5	0.5 ± 0.04	17.0±1.2
NaCl	0-1.0 M	-15.2 ± 0.2	--	--
$NaNO_3$	0-1.0 M	10.93 ± 0.8	1.8 ± 0.2	18.2 ± 5.0
NaH_2PO_4	0-1.0 M	-37.9 ± 0.2	--	--
Na_2SO_4	0-1.0 M	-72.1 ± 0.9	--	--
$NaClO_4$	0-1.0 M	7.08 ± 1.4	0.56 ±0.09	19.9± 3.2
Na_2CO_3	0-1.0 M	-70.2 ± 1.5	--	--

3.4.2. ^{1}H-NMR Measurements: Probing the Whole Polymer & Hydrophobic Interaction Mechanism

The effect of salts as a function of salt concentration with sugar macromolecules was monitored by ^{1}H-NMR spectroscopy. Two representative sodium salts were employed (NaSCN, NaCl) to probe the interactions. To elucidate the interaction of weakly hydrated anions with hydroxypropyl cellulose ^{1}H-NMR spectra of HPC in D_2O at 25℃ was taken as shown in Figure 27. The different types of protons are labeled based on the different chemical environments around them.

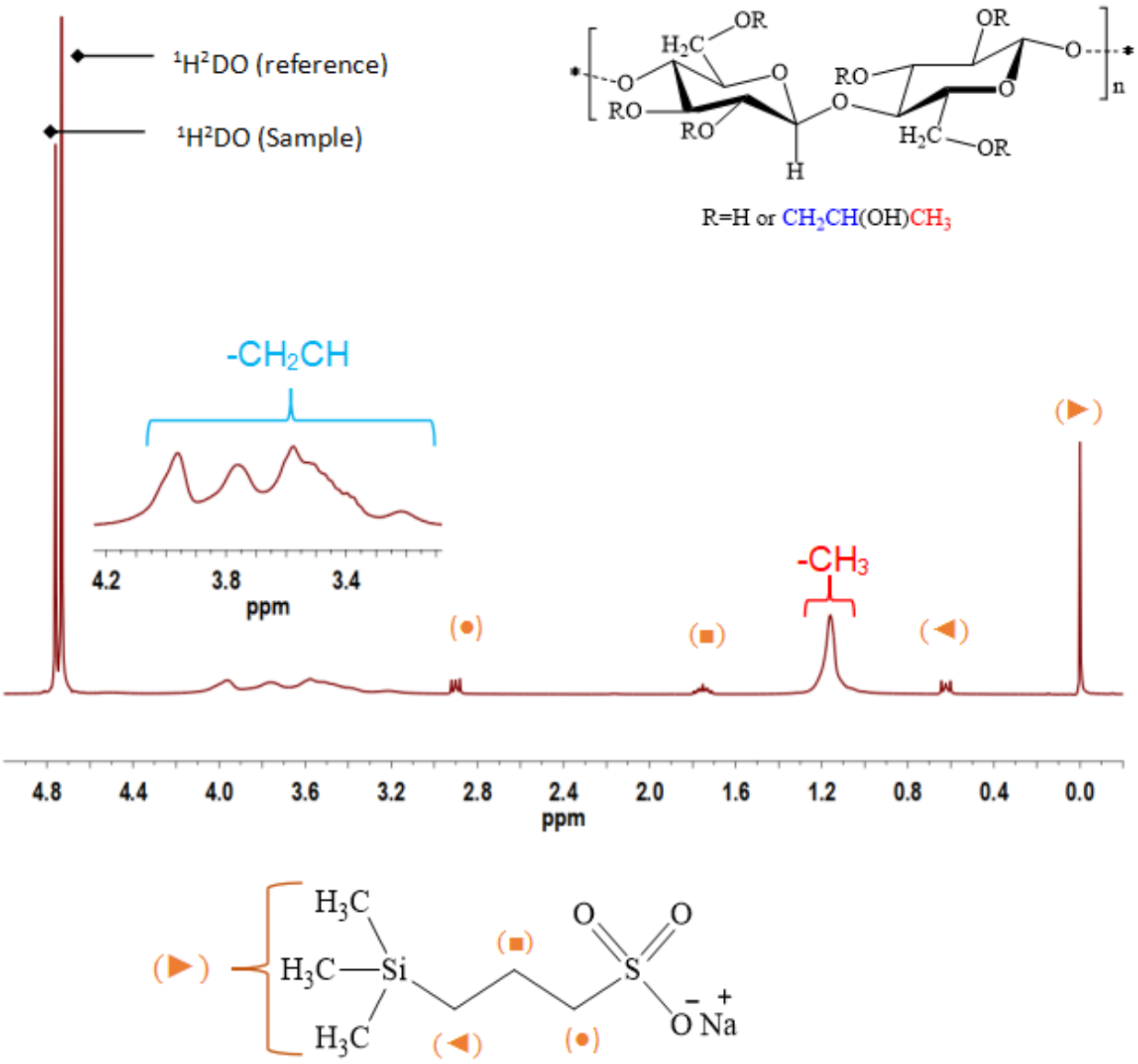

Figure 27: A representative ^1H-NMR spectra of Hydroxypropyl cellulose (HPC) in D_2O, obtained by external referencing to DSS. At the top, HPC structure is depicted with highlighting in different color for its signals. The structure of DSS is given below the spectra with color-coded set of H's corresponding to four resonance, as color-coded in spectra as well. Additionally, two different solvent peak :$^1H^2DO$ in sample and reference are labeled. Specific peak position are mentioned in the text for all components.

As it can be seen from the spectra the methyl group highlighted in red appears as a sharp singlet at 1.16 ppm. The methylene and methyne group from backbone as well as from side chain (-CH,-

CH_2) are all appear in downfield region of the spectra as multiplet at 3.1-4.1 ppm. The hydroxyl proton cannot be observed because of H-D exchange in solution with D_2O.

To elucidate the interaction of weekly hydrated anions to HPC, we investigated the effect of the addition of different concentrations of anions (0-1M) on the ^{1}H-NMR spectra of HPC. The nature of the interaction was determined from changes in the solute's proton chemical shifts, δ of the methyl at position (-CH_3) highlighted in red and methylene and methyne in region 3.1-4.1 ppm demonstrated as inset in spectra of HPC. The linear decrease in chemical shift for methyl protons at 1.16 ppm has been observed in case of both strongly and weakly hydrated anions. While the region for from 3.1-4.1 ppm for methyne and methylene protons is extracted and plotted separately in Figures 28 and 29 as a function of salt concentration. As we can see from the Figure 28 in case of Strongly hydrated anion (Cl^-) there is a linear decrease in chemical shift (deshielded $\delta_{downfield}$) values for all proton peaks with increasing salt (NaCl) concentration from 0-1 M. The linear decrease in chemical shift for all concentrations of salts is in accordance with the linear decrease in phase transition temperature (LCST) values for the corresponding salts in Figure 23. As a result, these values of the linearly decreasing proton chemical shift are consistent with the hypothesis well explained for amide-based polymers[41] that the ions do not interact with the macromolecules very strongly. In fact, it is believed that the ions are depleted at the macromolecule/water interface as a result of the salting out mechanism in Figure 28.

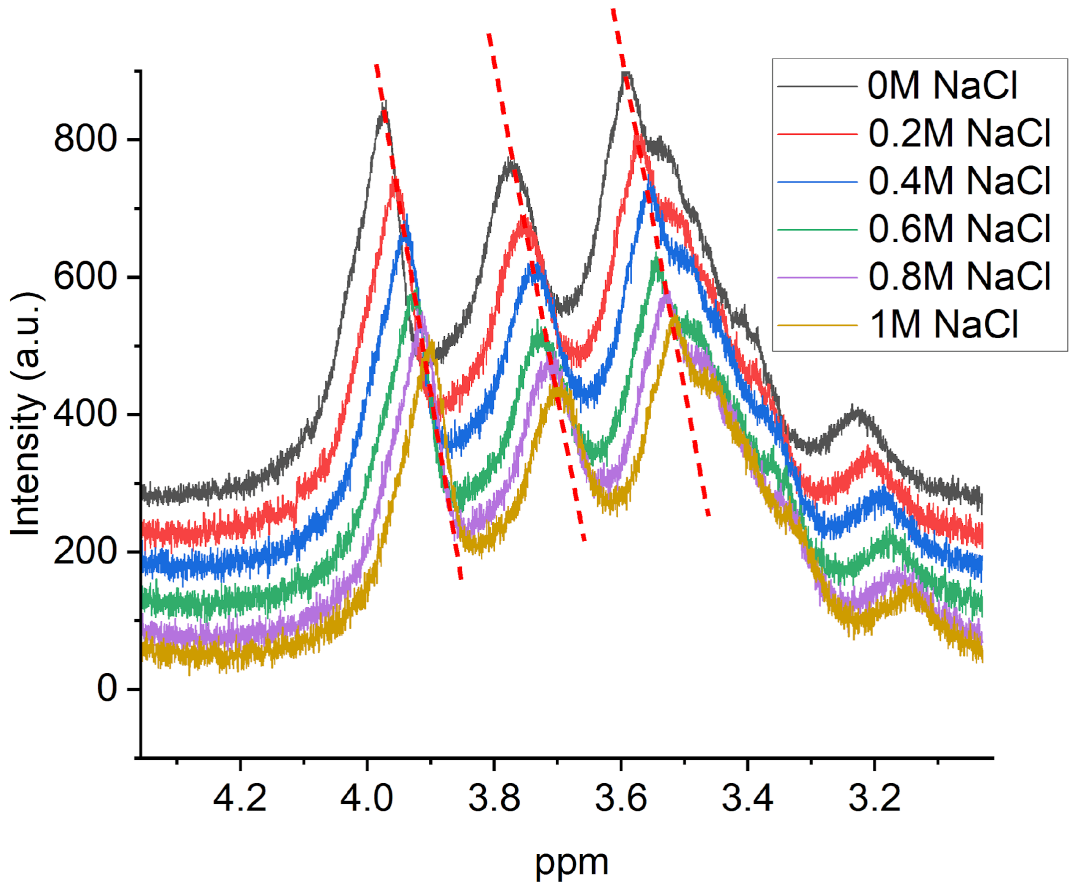

Figure 28: The shift of the normalized -$CHCH_2$ signals within size chain which was initially located at approximately 3.97ppm, 3.77ppm, 3.58ppm (from left to right for main peaks with tracking dashed line) with increasing concentration of NaCl. The spectra are offset according to concentration given in legend on right side of spectra. Tracking curve and approximate peak positions are incorporated as a guide to eye to help in interpretation.

whereas in case of weakly hydrated salt (NaSCN) as we can seen from the figure highlighted with dashed lines that chemical shift for all other peaks is decreasing while for peaks in the region from 3.4-3.6 ppm, at first there is a small increase in chemical shift (an upfield shift $\delta_{upfield}$) for low concentration of salt and then there is decrease in chemical shift towards (deshielded $\delta_{downfield}$) region of the spectra. In contrast to the data above mentioned for strongly hydrated anions, in the case of weakly hydrated anions, the trend for chemical shift values is not linear, instead, it first exhibits Langmuir-type binding behavior up to 0.2 M and after saturation, it starts increasing. Such non-linearity is in accordance with the binding interaction between these ions and HPC at this site. This result is consistent with the previous studies on amide-based polymers. In this case,

unfortunately this region is not obvious to us because from this region we cannot conclude that which protons (-CH, CH_2) either from back bone of HPC or from side chain of Hydroxypropyl correspond to chemical shift for this specific peak.

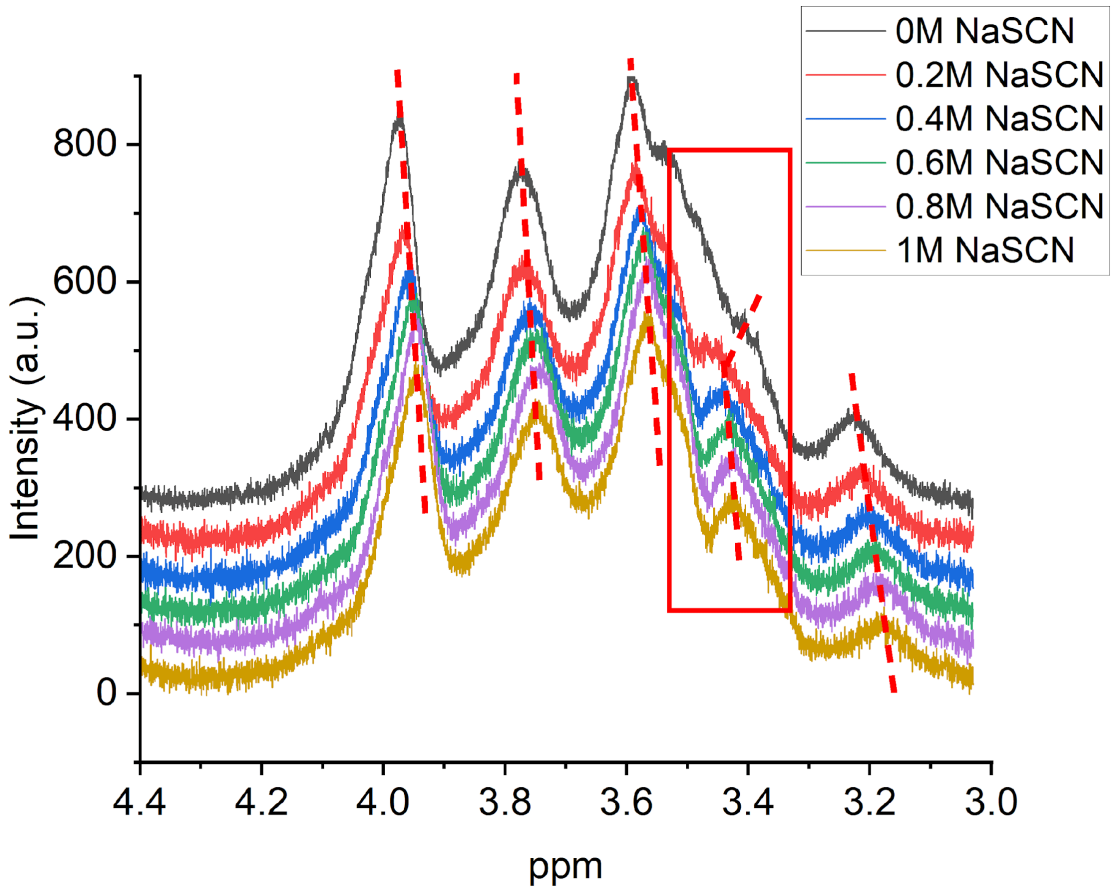

Figure 29: The shift of the normalized -$CHCH_2$ signals within size chain which were present initially roughly at 3.97 ppm, 3.77 ppm, 3.59 ppm (from left to right for main peaks with tracking dashed line) with increasing concentration of NaSCN. The spectra are offset according to concentration given in legend on right side of spectra. Tracking curve and approximate peak positions are incorporated as a guide to eye to help in interpretation. The area highlighted in rectangular box correspond to region where chemical shift instead of decreasing is increasing. (also demonstrated by tracking lines). This enclose section aim to draw attention to that it might be the site where SCN^- preferably binds. But it is clear that this is the site responsible for interaction between the weakly hydrated anions and the HPC and it can also be seen in LCST of HPC as a function of NaSCN. To further elucidate this region we performed 2D-NMR spectroscopy COSY.

3.4.3. 2D COSY NMR Measurements - Correlating Protons Coupling for Structural Insights.

In order to get the more detail about coupling of protons of HPC , COSY spectra was taken in D_2O at 25^0C as shown in figure.

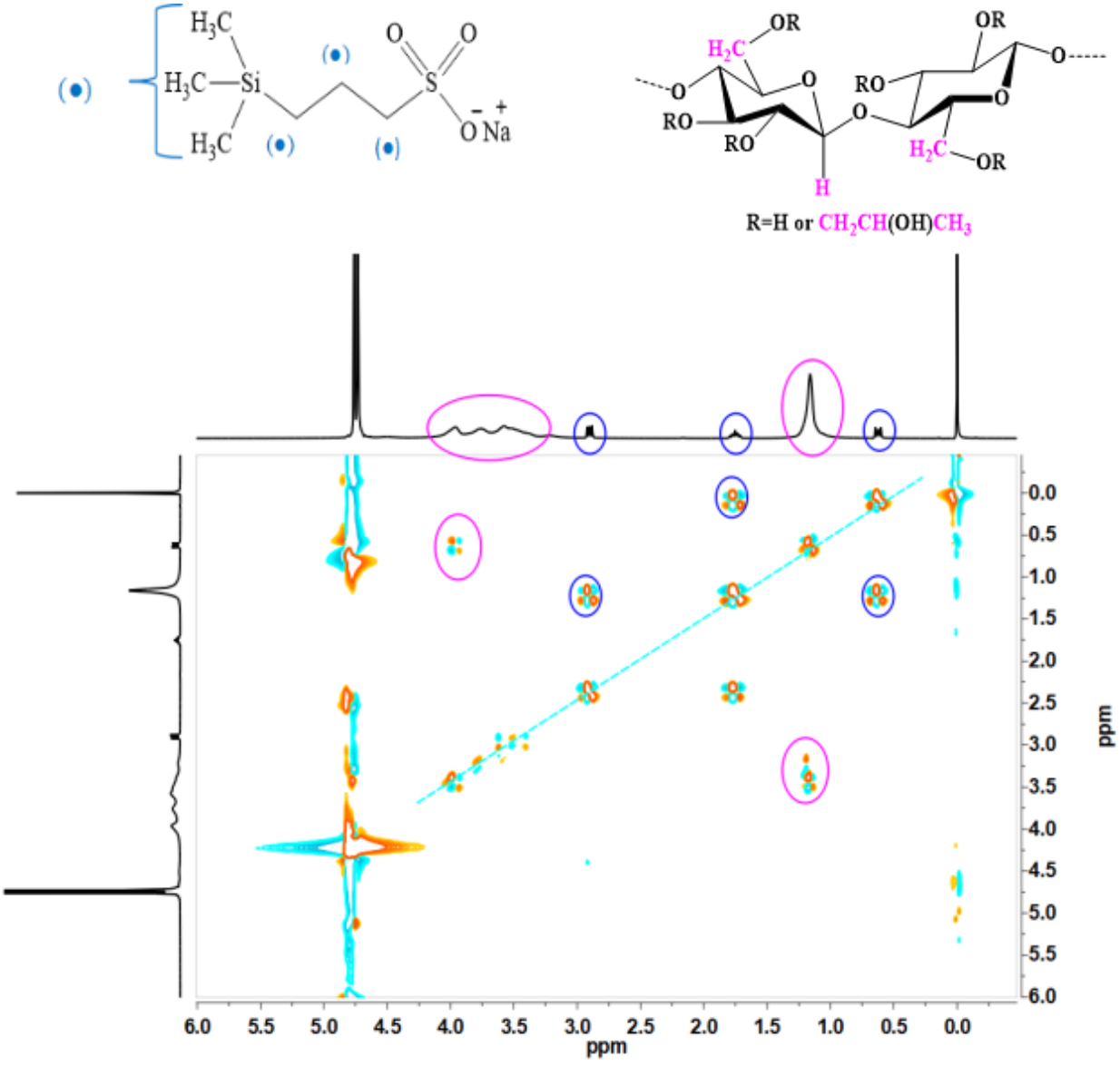

Figure 30: 2D-COSY NMR spectra of HPC in D_2O: The peaks encircle in purple color correspond to protons in HPC as highlighted in same color in structure of HPC given at top right of spectra. The spectra was obtained referencing with DSS, for which structure is given at top left corner of spectra and peak are encircled with blue color for all different protons of DSS.

The diagonal peaks marked by line does not provide any information about sample. The cross peaks are important to elucidate the information about coupling of protons. The peaks encircled in blue represent reference sample protons, while the peaks encircled in purple at 1.16 ppm(-CH_3) and from 3.1-4.1 ppm (CH, CH_2) corresponds to HPC protons. As can be seen from the spectra the cross peak for -CH_3 have coupling with peaks from -CH, and -CH_2, which indicates that these peaks are from side chain of HPC because COSY gives the coupling of protons that are two, three or four bonds are apart but if we look at the chemical structure of HPC backbone -CH and -CH_2 are more than four bonds apart so coupling between side chain and backbone protons cannot be demonstrated by COSY.

3.5. SUMMARY: Sugar macromolecule (HPC) and interaction with Hofmeister Anions.

In the second part of this thesis, the focus was on investigating the interaction of Hofmeister anions with macromolecules beyond the amide-based ones. As such, sugar-based macromolecules were introduced using HPC as a model molecule. Two different methods, phase transition temperature measurements and ^{1}H-NMR were employed to get molecular level insight into the nature of ion interactions with such systems. It was found that the strongly hydrated anions such as Cl^- show no binding behavior while the data suggests that the weakly hydrated anions (SCN^-) prefer to weakly interact with the side chain groups of hydroxypropyl cellulose macromolecules.

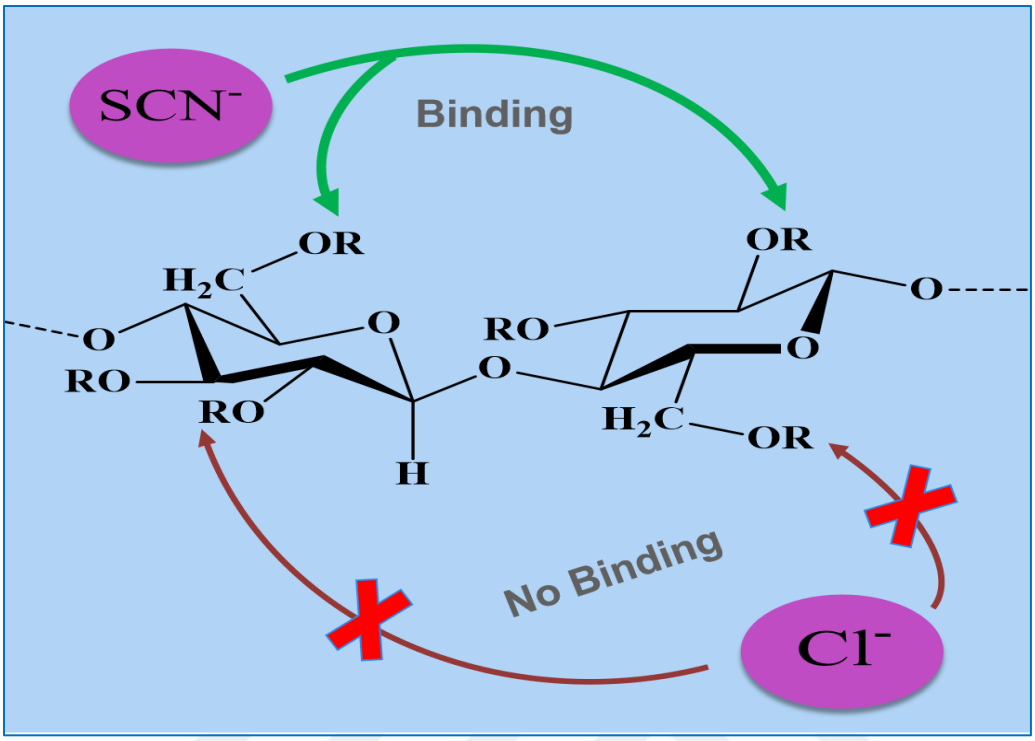

Figure 31: Pictorial representation of the main summary of second part of present work: the molecular mechanism underlying the binding and non-binding of weakly hydrated (SCN^-) and strongly hydrated (Cl^-) anions on Hydroxypropyl cellulose (HPC). The anion SCN^- demonstrate weak binding while Cl^- shows non-binding to HPC.

Chapter 4-Conclusion

Over a century ago, Franz Hofmeister arranged ions in a series based on their ability to precipitate proteins from aqueous solution. Since then, scientists have dedicated considerable efforts to unravel the molecular level complexities of the Hofmeister effect and mechanism underlying this phenomenon. Numerous models such as direct ion binding, preferential hydration, and protein surface charge density hypothesis, each proposing distinct mechanisms have been formulated to comprehend ion specific effects. Many physiological biomolecules such as proteins, biopolymers, sugars, ATP and amino acids have been studied to understand the Hofmeister effect. Despite decades of dedicated research there is still much to explore in the wide variety of the specific ion effects.

In this thesis, we explored the influence of specific ion effects on the thermoresponsive oligomers of PNIPAM. To study this effect PNIPAM oligomers were synthesized by radical and RAFT polymerization methods. The oligomers were synthesized with different end groups i.e. charged and neutral end groups based on two different types of initiators used during polymerization. These oligomers were characterized by LCST and ^{1}H-NMR spectroscopy measurements. The synthesized oligomers were utilized to explore the molecular size effect on ion - macromolecule interactions.

Moreover, the Hofmeister effect on sugar-based macromolecules, i.e. hydroxypropyl cellulose (HPC) were elucidated. Eight different sodium salts (NaSCN, NaI, $NaNO_3$, $NaClO_4$, NaCl, Na_2SO_4, Na_2CO_3, NaH_3PO_4) were employed. It has been demonstrated that the specific ion effects on the phase transition temperature behavior of HPC is reminiscent of the phase transition behavior of amide-based polymers. Strongly hydrated anions monotonically decrease the phase transition temperature, while the weakly hydrated anions yield a non-monotonic trend as a function of salt concentration. The ion binding mechanism was studied by ^{1}H-NMR spectroscopy for two representative salts NaCl and NaSCN. Although the actual binding side cannot be ruled out, it was concluded that the apparent ion binding occurs at the side chain of the sugar-based macromolecule.

References

1. Warren, J. C., & Cheatum, S. G. Effect of neutral salts on enzyme activity and structure. *Biochemistry*, **5**, 1702-1707 (1966).

2. Hayashi, M., Unemoto, T., & Hayashi, M. pH-and anion-dependent salt modifications of alkaline phosphatase from a slightly halophilic Vibrio alginolyticus. *Biochimica et Biophysica Acta (BBA)-Enzymology*, **315**, 83-93 (1973).

3. Štěpánková, V., Paterová, J., Damborský, J., Jungwirth, P., Chaloupková, R., & Heyda, J. Cation-specific effects on enzymatic catalysis driven by interactions at the tunnel mouth. *The Journal of Physical Chemistry B*, **117**, 6394-6402 (2013).

4. Garajová, K., Balogová, A., Dušeková, E., Sedláková, D., Sedlák, E., & Varhač, R. Correlation of lysozyme activity and stability in the presence of Hofmeister series anions. *Biochimica et Biophysica Acta (BBA)-Proteins and Proteomics*, **1865**, 281-288 (2017)..

5. Wright, E. M., & Diamond, J. M. Anion selectivity in biological systems. *Physiological Reviews*, ***57***, 109-156 (1977).

6. Cacace, M. G., Landau, E. M., & Ramsden, J. J. The Hofmeister series: salt and solvent effects on interfacial phenomena. *Quarterly reviews of biophysics*, **30**, 241-277 (1997).

7. Wang, Q. M., & Johnson, R. B. Activation of human rhinovirus-14 3C protease. *Virology*, **280**, 80-86 (2001).

8. Salis, A., Bilanicˇova, D., Ninham, B. W., & Monduzzi, M. Hofmeister effects in enzymatic activity: weak and strong electrolyte influences on the activity of Candida rugosa lipase. *The Journal of Physical Chemistry B*, **111**, 1149-1156 (2007).

9. Bilanicová, D., Salis, A., Ninham, B. W., & Monduzzi, M. Specific anion effects on enzymatic activity in non aqueous media. *The Journal of Physical Chemistry B*, **112**, 12066-12072 (2008).

10. Zhang, Y., & Cremer, P. S. The inverse and direct Hofmeister series for lysozyme. *Proceedings of the National Academy of Sciences*, **106**, 15249-15253 (2009).

11. Carucci, C., Raccis, F., Salis, A., & Magner, E. Specific ion effects on the enzymatic activity of alcohol dehydrogenase from Saccharomyces cerevisiae. *Physical Chemistry Chemical Physics*, **22**, 6749-6754 (2020).

12. Collu, M., Carucci, C., & Salis, A. Specific anion effects on lipase adsorption and enzymatic synthesis of biodiesel in nonaqueous media. *Langmuir*, **36**, 9465-9471 (2020).

13. Somasundar, A., Ghosh, S., Mohajerani, F., Massenburg, L. N., Yang, T., Cremer, P. S., ... & Sen, A. Positive and negative chemotaxis of enzyme-coated liposome motors. *Nature nanotechnology*, **14**, 1129-1134 (2019).

14. Lo Nostro, P., & Ninham, B. W. Hofmeister phenomena: an update on ion specificity in biology. *Chemical reviews*, **112**, 2286-2322 (2012).

15. Coso, J. D., Estevez, E., Baquero, R. A., & Mora-Rodriguez, R. Anaerobic performance when rehydrating with water or commercially available sports drinks during prolonged exercise in the heat. *Applied Physiology, Nutrition, and Metabolism*, **33**, 290-298 (2008).

16. F. Hofmeister, Zur Lehre Von Der Wirkung Der Salze, Naunyn-Schmiedeberg's Arch. Pharmacol., **24**, 247 (1888).

17. Kunz, W., Henle, J. W. N. B., & Ninham, B. W. 'Zur Lehre von der Wirkung der Salze'(about the science of the effect of salts): Franz Hofmeister's historical papers. *Current Opinion in Colloid & Interface Science*, **9**, 19-37 (2004).

18. dos Santos, A. P., Diehl, A., & Levin, Y. . Surface tensions, surface potentials, and the Hofmeister series of electrolyte solutions. *Langmuir*, **26**, 10778-10783 (2010).

19. Wojciechowski, K., Bitner, A., Warszyński, P., & Żubrowska, M. The Hofmeister effect in zeta potentials of CTAB-stabilised toluene-in-water emulsions. *Colloids and Surfaces A: Physicochemical and Engineering Aspects*, **376**, 122-126 (2011).

20. Cugia, F., Sedda, S., Pitzalis, F., Parsons, D. F., Monduzzi, M., & Salis, A. Are specific buffer effects the new frontier of Hofmeister phenomena? Insights from lysozyme adsorption on ordered mesoporous silica. *RSC advances*, **6**, 94617-94621 (2016).

21. Heyda, J., & Dzubiella, J. Thermodynamic description of Hofmeister effects on the LCST of thermosensitive polymers. *The Journal of Physical Chemistry B*, **118**, 10979-10988 (2014).

22. Shechter, I., Ramon, O., Portnaya, I., Paz, Y., & Livney, Y. D. Microcalorimetric study of the effects of a chaotropic salt, KSCN, on the lower critical solution temperature (LCST) of aqueous poly (N-isopropylacrylamide)(PNIPAM) solutions. *Macromolecules*, **43**, 480-487 (2010)..

23. Zhang, Y., Furyk, S., Sagle, L. B., Cho, Y., Bergbreiter, D. E., & Cremer, P. S. Effects of Hofmeister anions on the LCST of PNIPAM as a function of molecular weight. *The Journal of Physical Chemistry C*, **111**, 8916-8924 (2007).

24. Collins, K. D. Ions from the Hofmeister series and osmolytes: effects on proteins in solution and in the crystallization process. *Methods*, **34**, 300-311 (2004).

25. Boström, M., Williams, D. R. M., Stewart, P. R., & Ninham, B. W. Hofmeister effects in membrane biology: the role of ionic dispersion potentials. *Physical Review E*, **68**, 041902 (2003).

26. Davis, A. P., Sheppard, D. N., & Smith, B. Development of synthetic membrane transporters for anions. *Chemical Society Reviews*, **36**, 348-357 . (2007). .

27. Ninham, B. W., & Yaminsky, V. (Ion binding and ion specificity: the Hofmeister effect and Onsager and Lifshitz theories. *Langmuir*, **13**, 2097-2108 (1997).

28. Boström, M., Tavares, F. W., Finet, S., Skouri-Panet, F., Tardieu, A., & Ninham, B. W. Why forces between proteins follow different Hofmeister series for pH above and below pI. *Biophysical chemistry*, **117**, 217-224 (2005).

29. Abezgauz, L., Kuperkar, K., Hassan, P. A., Ramon, O., Bahadur, P., & Danino, D.Effect of Hofmeister anions on micellization and micellar growth of the surfactant cetylpyridinium chloride. *Journal of colloid and interface science*, **342**, 83-92 (2010). .

30. Cox, W. M., & Wolfenden, J. H. The viscosity of strong electrolytes measured by a differential method. *Proceedings of the Royal Society of London. Series A, Containing Papers of a Mathematical and Physical Character*, **145**, 475-488 (1934).

31. Jones, G., & Dole, M.. The viscosity of aqueous solutions of strong electrolytes with special reference to barium chloride. *Journal of the American Chemical Society*, **51**, 2950-2964 (1929).

32. Zavitsas, A. A. Properties of water solutions of electrolytes and non electrolytes. *The Journal of Physical Chemistry B*, **105**, 7805-7817 (2001).

33. Marcus, Y. *Ions in Solution and their Solvation*. John Wiley & Sons (2015).

34. Holm, G. E., & Sherman, J. M. SALT EFFECTS IN BACTERIAL GROWTH I. PRELIMINARY PAPER. *Journal of bacteriology*, ***6***, 511-519 (1921).

35. Henry, C. L., & Craig, V. S.The link between ion specific bubble coalescence and Hofmeister effects is the partitioning of ions within the interface. *Langmuir*, ***26***, 6478-6483 (2010).

36. Melander, W., & Horváth, C. Salt effects on hydrophobic interactions in precipitation and chromatography of proteins: an interpretation of the lyotropic series. *Archives of biochemistry and biophysics*, **183**, 200-215 (1977).

37. Graziano, G. Salting out of methane by sodium chloride: a scaled particle theory study. *The Journal of chemical physics*, **129** (2008).

38. Pica, A., & Graziano, G. On the effect of sodium salts on the coil-to-globule transition of poly (N-isopropylacrylamide). *Physical Chemistry Chemical Physics*, **17**, 27750-27757 (2015).

39. Pica, A., & Graziano, G. Effect of sodium thiocyanate and sodium perchlorate on poly (N-isopropylacrylamide) collapse. *Physical Chemistry Chemical Physics*, **22**, 189-195 (2020).

40. Baldwin, R. L. How Hofmeister ion interactions affect protein stability. *Biophysical journal*, **71**, 2056-2063 (1996).

41. Rogers, B. A., Okur, H. I., Yan, C., Yang, T., Heyda, J., & Cremer, P. S. Weakly hydrated anions bind to polymers but not monomers in aqueous solutions. *Nature Chemistry*, **14**, 40-45 (2022).

42. Collins, K. D. Charge density-dependent strength of hydration and biological structure. *Biophysical journal*, **72**, 65-76 (1997).

43. Leberman, R., & Soper, A. K. Effect of high salt concentrations on water structure. *Nature*, **378**, 364-366 (1995).

44. Waluyo, I., Nordlund, D., Bergmann, U., Schlesinger, D., Pettersson, L. G., & Nilsson, A. A different view of structure-making and structure-breaking in alkali halide aqueous solutions through x-ray absorption spectroscopy. *The Journal of Chemical Physics*, **140**, (2014).

45. Tielrooij, K. J., Garcia-Araez, N., Bonn, M., & Bakker, H. J. Cooperativity in ion hydration. *science*, **328**, 1006-1009 (2010).

46. Parsegian, V. A. *Van der Waals forces: a handbook for biologists, chemists, engineers, and physicists*. Cambridge University Press (2005).

47. Born, M.. Volumen und hydratationswärme der ionen. *Zeitschrift für physik*, **1**, 45-48 (1920).

48. Mayer, U., & Gutmann, V. Phenomenological approach to cation-solvent interactions. In *Structure and Bonding*. Berlin, Heidelberg: Springer Berlin Heidelberg.113-140, (2007).

49. P. Debye and E. Hu¨ckel, Debye–Hu¨ckel theory of electrolytes, *Phys. Z.*, **24**, 185 (1923).

50. Derjaguin, B., & Landau, L. Theory of the stability of strongly charged lyophobic sols and of the adhesion of strongly charged particles in solutions of electrolytes. *Progress in Surface Science*, **43**, 30-59(1993)..

51. Verwey, E. J. W. . Theory of the stability of lyophobic colloids. *The Journal of Physical Chemistry*, **51**, 631-636 (1947).

52. Verwey, E. J. W., & Overbeek, J. T. G. Theory of the stability of lyophobic colloids. *Journal of Colloid Science*, **10**, 224-225 (1955).

53. Pitzer, K. S. Thermodynamics of electrolytes. I. Theoretical basis and general equations. *The Journal of Physical Chemistry*, **77**, 268-277 (1973).

54. Heyrovska, R. . Physical electrochemistry of strong electrolytes based on partial dissociation and hydration: quantitative interpretation of the thermodynamic properties of NaCl (aq) from "zero to saturation". *Journal of the Electrochemical Society*, **143**, 1789 (1996).

55. Collins, K. D., & Washabaugh, M. WThe Hofmeister effect and the behaviour of water at interfaces. *Quarterly reviews of biophysics*, **18**, 323-422 (1985).

56. Leontidis, E. Investigations of the Hofmeister series and other specific ion effects using lipid model systems. *Advances in Colloid and Interface Science*, **243**, (2017)..

57. Mazzini, V., & Craig, V. S. What is the fundamental ion-specific series for anions and cations? Ion specificity in standard partial molar volumes of electrolytes and electrostriction in water and non-aqueous solvents. *Chemical science*, **8**, 7052-7065 (2017).

58. Stone, A.The theory of intermolecular forces. *oUP oxford* (2013).

59. Parsons, D. F., & Ninham, B. W. Ab initio molar volumes and Gaussian radii. *The Journal of Physical Chemistry A*, **113**, 1141-1150 (2009).

60. Fridovich, I. Inhibition of acetoacetic decarboxylase by anions: the Hofmeister lyotropic series. *Journal of Biological Chemistry*, **238**, 592-598 (1963).

61. Collins, K. D., Neilson, G. W., & Enderby, J. E. Ions in water: Characterizing the forces that control chemical processes and biological structure. *Biophysical chemistry*, **128,** 95-104 (2007).

62. Doyle, D. A., Cabral, J. M., Pfuetzner, R. A., Kuo, A., Gulbis, J. M., Cohen, S. L., ... & MacKinnon, R. The structure of the potassium channel: molecular basis of K+ conduction and selectivity. *science*, **280**, 69-77 (1998).

63. Hille, B., Armstrong, C. M., & MacKinnon, R. Ion channels: from idea to reality. *Nature medicine*, **5**, 1105-1109 (1999).

64. Dabrowa, K., Ulatowski, F., Lichosyt, D., & Jurczak, J. Catching the chloride: searching for non-Hofmeister selectivity behavior in systematically varied polyamide macrocyclic receptors. *Organic & Biomolecular Chemistry*, **15**, 5927-5943 (2017).

65. Gregory, K. P., Wanless, E. J., Webber, G. B., Craig, V. S., & Page, A. J. The electrostatic origins of specific ion effects: quantifying the Hofmeister series for anions. *Chemical Science*, **12**, 15007-15015 (2021).

66. Marcus, Y. The thermodynamics of solvation of ions. Part 4.—Application of the tetraphenylarsonium tetraphenylborate (TATB) extrathermodynamic assumption to the hydration of ions and to properties of hydrated ions. *Journal of the Chemical Society, Faraday Transactions 1: Physical Chemistry in Condensed Phases*, **83**, 2985-2992 (1987).

67. Ball, P. . Chemical physics: How to keep dry in water. *Nature*, **423**, 25-27 (2003).

68. Israelachvili, J., & Wennerström, HRole of hydration and water structure in biological and colloidal interactions. *Nature*, **379**, 219-225 (1996). .

69. Enderby, J. E., & Neilson, G. W. Water, a comprehensive treatise. *by F. Franks, Plenum Press, New York*, **6**, 1 (1979).

70. Mitsui, T., M. K. Rose, E. Fomin, and M. Salmeron. "Water diffusion and clustering on Pd (111)." *Science*, **297**, 1850-1852 (2002).

71. Cerdá, J., A. Michaelides, M-L. Bocquet, Peter J. Feibelman, E. Fomin, and M. Salmeron. "Novel water overlayer growth on Pd (111) characterized with scanning tunneling microscopy and density functional theory." *Physical review letters*, **93**, 116101 (2004) .

72. Tieke, B., K. U. Fulda, and A. Kampes. "In Nano-Surface Chemistry; Rosoff, M., Ed.; Mono-and Multilayers of Spherical Polymer Particles Prepared by Langmuir-Blodgett and Self-Assembly Techniques." **213**, (2002).

73. Devi, Reena, Sunita Srivastava, and K. Tankeshwar. "Dynamics of Fluids Contained in a Nano-cube." *Nano Biomedicine & Engineering* 3, **1** (2011).

74. Ghosal, S., Hemminger, J. C., Bluhm, H., Mun, B. S., Hebenstreit, E. L., Ketteler, G., ... & Salmeron, M. Electron spectroscopy of aqueous solution interfaces reveals surface enhancement of halides. *Science*, **307,** 563-566 (2005).

75. Wilson, K. R., Rude, B. S., Smith, J., Cappa, C., & Saykally, R. J.Investigation of volatile liquid surfaces by synchrotron x-ray spectroscopy of liquid microjets. *Review of Scientific Instruments*, **75**, 725-736 (2004).

76. Reedijk, M. F., Arsic, J., Hollander, F. F. A., De Vries, S. A., & Vlieg, E. Liquid order at the interface of KDP crystals with water: evidence for icelike layers. *Physical review letters*, **90**, 066103 (2003).

77. Jensen, T. R., Jensen, M. Ø., Reitzel, N., Balashev, K., Peters, G. H., Kjaer, K., & Bjørnholm, T. Water in contact with extended hydrophobic surfaces: direct evidence of weak dewetting. *Physical review letters*, **90**, 086101 (2003).

78. Steitz, R., Gutberlet, T., Hauss, T., Klösgen, B., Krastev, R., Schemmel, S., ... & Findenegg, G. H. Nanobubbles and their precursor layer at the interface of water against a hydrophobic substrate. *Langmuir*, **19**, 2409-2418 (2003).

79. Richmond, G. L. Molecular bonding and interactions at aqueous surfaces as probed by vibrational sum frequency spectroscopy. *Chemical reviews*, **102**, 2693-2724 (2002).

80. Prather, K. A., Bertram, T. H., Grassian, V. H., Deane, G. B., Stokes, M. D., DeMott, P. J., ... & Zhao, D. Bringing the ocean into the laboratory to probe the chemical complexity of sea spray aerosol. *Proceedings of the National Academy of Sciences*, **110**, 7550-7555 (2013).

81. Rogers, M. M., Neal, J. F., Saha, A., Algarni, A. S., Hill, T. C., & Allen, H. C. The Ocean's Elevator: Evolution of the Air–Seawater Interface during a Small-Scale Algal Bloom. *ACS Earth and Space Chemistry*, **12**, 2347-2357 (2020).

82. Rana, B., Fairhurst, D. J., & Jena, K. C. Ion-Specific Water–Macromolecule Interactions at the Air/Aqueous Interface: An Insight into Hofmeister Effect. *Journal of the American Chemical Society*, **145**, 9646-9654 (2023).

83. Zhang, Y., & Cremer, P. S. . Interactions between macromolecules and ions: the Hofmeister series. *Current opinion in chemical biology*, **10**, 658-663 (2006).

84. Kalra, A., Tugcu, N., Cramer, S. M., & Garde, S. Salting-in and salting-out of hydrophobic solutes in aqueous salt solutions. *The Journal of Physical Chemistry B*, **105,** 6380-6386 (2001).

85. Shimizu, S., McLaren, W. M., & Matubayasi, N. The Hofmeister series and protein-salt interactions. *The Journal of chemical physics*, **124**, (2006).

86. Tavares, F. W., Bratko, D., & Prausnitz, J. M. The role of salt–macroion van der Waals interactions in the colloid–colloid potential of mean force. *Current opinion in colloid & interface science*, **9**, 81-86 (2004).

87. Boström, M., Tavares, F. W., Finet, S., Skouri-Panet, F., Tardieu, A., & Ninham, B. W. Why forces between proteins follow different Hofmeister series for pH above and below pI. *Biophysical chemistry*, **117**, 217-224 (2005).

88. Jungwirth, P., & Tobias, D. J. Specific ion effects at the air/water interface. *Chemical reviews*, **106**, 1259-1281 (2006).

89. Huang, D. M., Cottin-Bizonne, C., Ybert, C., & Bocquet, L. Ion-specific anomalous electrokinetic effects in hydrophobic nanochannels. *Physical review letters*, **98**, 177801 (2007).

90. Jagoda-Cwiklik, B., Vácha, R., Lund, M., Srebro, M., & Jungwirth, P. Ion pairing as a possible clue for discriminating between sodium and potassium in biological and other complex environments. *The Journal of Physical Chemistry B*, **111**, 14077-14079 (2007).

91. Vrbka, L., Vondrášek, J., Jagoda-Cwiklik, B., Vácha, R., & Jungwirth, P.Quantification and rationalization of the higher affinity of sodium over potassium to protein surfaces. *Proceedings of the National Academy of Sciences*, **103,** 15440-15444 (2006).

92. Lund, M., Vácha, R., & Jungwirth, P. Specific ion binding to macromolecules: effects of hydrophobicity and ion pairing. *Langmuir*, **24**, 3387-3391 (2008).

93. Lo Nostro, P. & Ninham, B. W. Hofmeister Phenomena: An Update on Ion Specificity in Biology. *Chem Rev*, **112**, 2286–2322 (2012)

94. Roy, D., Brooks, W. L. A. & Sumerlin, B. S. New directions in thermoresponsive polymers. *Chem Soc Rev*, **42**, 7214–7243 (2013).

95. Tiktopulo, E. I. *et al.* 'Domain' Coil-Globule Transition in Homopolymers. *Macromolecules*, **28**, 7519–7524 (1995)

96. Zhang, Y. & Cremer, P. S. Interactions between macromolecules and ions: the Hofmeister series. *Curr Opin Chem Biol*, **10**, 658–663 (2006).

97. Von Hippel, P. H., Peticolas, V., Schack, L. & Karlson, L. Model studies on the effects of neutral salts on the conformational stability of biological macromolecules. I. Ion binding to polyacrylamide and polystyrene columns. *Biochemistry*, **12**, 1256–1264 (1973).

98. Song, J. D., Ryoo, R. & Jhon, M. S. Anion binding properties of poly(vinylpyrrolidone) in aqueous solution studied by halide NMR spectroscopy. *Macromolecules*, **24**, 1727–1730 (1991).

99. Breslow, R. & Guo, T. Surface tension measurements show that chaotropic salting-in denaturants are not just water-structure breakers. *Proceedings of the National Academy of Sciences*, **87**, 167–169 (1990).

100. Cho, Y. *et al.* Effects of Hofmeister Anions on the Phase Transition Temperature of Elastin-like Polypeptides. *J Phys Chem B,* **112**, 13765–13771 (2008).

101. Meyer, D. E. & Chilkoti, A. Quantification of the Effects of Chain Length and Concentration on the Thermal Behavior of Elastin-like Polypeptides. *Biomacromolecules,* **5**, 846–851 (2004).

102. Rembert, K. B., Paterová, J., Heyda, J., Hilty, C., Jungwirth, P., & Cremer, P. S. Molecular mechanisms of ion-specific effects on proteins. *Journal of the American Chemical Society*, **134**, 10039-10046 (2012).

103. Rembert, K. B., Okur, H. I., Hilty, C., & Cremer, P. S. An NH moiety is not required for anion binding to amides in aqueous solution. *Langmuir*, **31**, 3459-3464 (2015).

104. Okur, H. I., Hladílková, J., Rembert, K. B., Cho, Y., Heyda, J., Dzubiella, J., ... & Jungwirth, P. . Beyond the Hofmeister series: Ion-specific effects on proteins and their biological functions. *The Journal of Physical Chemistry B*, **121**, 1997-2014 (2017).

105. Collins, K. D. & Washabaugh, M. W. The Hofmeister effect and the behaviour of water at interfaces. *Q Rev Biophys,* **18**, 323–422 (1985)

106. Cacace, M. G., Landau, E. M. & Ramsden, J. J. The Hofmeister series: Salt and solvent effects on interfacial phenomena. *Q Rev Biophys,* **30**, 241–277 (1997).

107. Lo Nostro, P. & Ninham, B. W. Hofmeister Phenomena: An Update on Ion Specificity in Biology. *Chem Rev,* **112**, 2286–2322 (2012).

108. Zhang, Y. & Cremer, P. S. Chemistry of Hofmeister Anions and Osmolytes. *Annu Rev Phys Chem*, **61**, 63–83 (2010).

109. Jungwirth, P. & Tobias, D. J. Specific ion effects at the air/water interface. *Chem Rev*, **106**, 1259–1281 (2006)

110. Jungwirth, P. & Tobias, D. J. Ions at the Air/Water Interface. *J Phys Chem B*, **106**, 6361–6373 (2002).

111. Ghosal, S. *et al.* Electron Spectroscopy of Aqueous Solution Interfaces Reveals Surface Enhancement of Halides. *Science,* **307**, 563–566 (2005).

112. Collins, K. D., Neilson, G. W. & Enderby, J. E. Ions in water: Characterizing the forces that control chemical processes and biological structure. *Biophys Chem*, **128**, 95–104 (2007).

113. Balos, V., Bonn, M. & Hunger, J. Quantifying transient interactions between amide groups and the guanidinium cation. *Physical Chemistry Chemical Physics,* **17**, 28539–28543 (2015).

114. Balos, V., Bonn, M. & Hunger, J. Correction: Quantifying transient interactions between amide groups and the guanidinium cation. *Physical Chemistry Chemical Physics*, **18**, 1346–1347 (2016).

115. Bruce, E. E. *et al.* Molecular Mechanism for the Interactions of Hofmeister Cations with Macromolecules in Aqueous Solution. *J Am Chem Soc*, **142**, 19094–19100 (2020)

116. Paterová, J., Rembert, K. B., Heyda, J., Kurra, Y., Okur, H. I., Liu, W. R., ... & Jungwirth, P. Reversal of the Hofmeister series: specific ion effects on peptides. *The Journal of Physical Chemistry B*, **117**, 8150-8158 (2013).

117. H. I. Okur, J. Hladı´lkova´, K. B. Rembert, Y. Cho, J. Heyda, J. Dzubiella, P. S. Cremer and P. Jungwirth, Beyond the Hofmeister Series: Ion-Specific Effects on Proteins and Their Biological Functions, *J. Phys. Chem. B,* **121**, 1997–2014 (2017).

118. Sakr, S., Wang, M., Dédaldéchamp, F., Perez-Garcia, M. D., Ogé, L., Hamama, L., & Atanassova, R. The sugar-signaling hub: overview of regulators and interaction with the hormonal and metabolic network. *International journal of molecular sciences*, **19**, 2506 (2018).

119. Zhang, Y., Chan, J. W., Moretti, A., & Uhrich, K. E. Designing polymers with sugar-based advantages for bioactive delivery applications. *Journal of Controlled Release*, **219**, 355-368 (2015).

120. Sood, A., Gupta, A., & Agrawal, G. Recent advances in polysaccharides based biomaterials for drug delivery and tissue engineering applications. *Carbohydrate Polymer Technologies and Applications*, **2,** 100067 (2021).

121. Stillinger, F. H. Structure in aqueous solutions of nonpolar solutes from the standpoint of scaled-particle theory. In *The Physical Chemistry of Aqueous System: A Symposium in Honor of Henry S. Frank on His Seventieth Birthday*. Springer US, 43-60 (1973).

122. Zhang, Y., Furyk, S., Sagle, L. B., Cho, Y., Bergbreiter, D. E., & Cremer, P. S. Effects of Hofmeister anions on the LCST of PNIPAM as a function of molecular weight. *The Journal of Physical Chemistry C*, **111**, 8916-8924 (2007).

123. Zhang, Y., Furyk, S., Bergbreiter, D. E., & Cremer, P. S. Specific ion effects on the water solubility of macromolecules: PNIPAM and the Hofmeister series. *Journal of the American Chemical Society*, **127**, 14505-14510 (2005).